Fribourg University December, 5th, 2017

Quantifying paleostress : toward a better quantification of magnitudes of past stresses and fluid (over)pressures in sedimentary basins; insights from calcite twinning and stylolite roughness paleopiezometry

Olivier LACOMBE

Professor at Université Pierre et Marie Curie, Paris, France

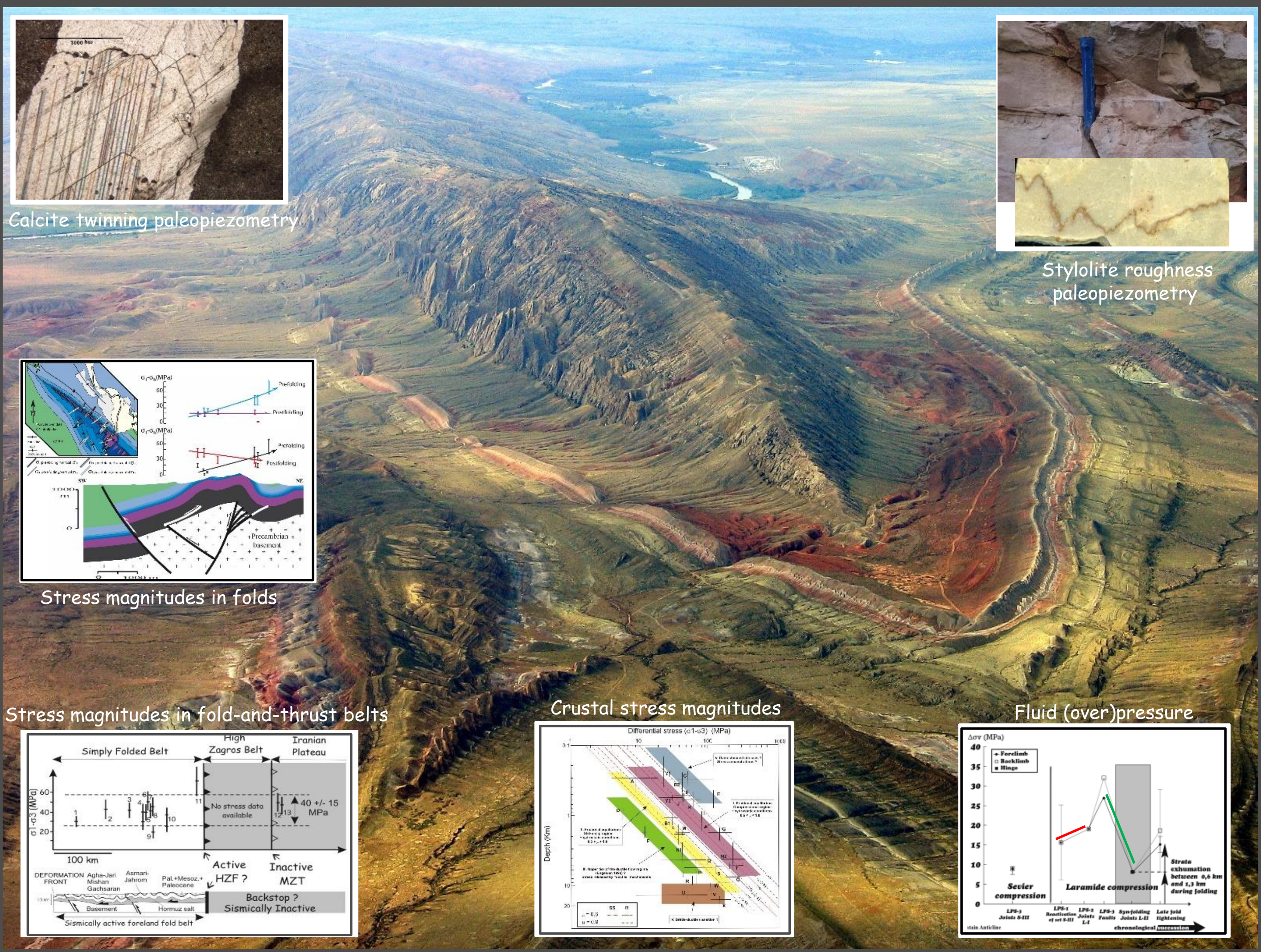

ISTeP Institut des Sciences de la Terre de Paris UMR 7193-UPMC-CNRS

UPMC SORBONNE UNIVERSITÉS

CNRS INSU Observer & comprendre

Fribourg, 12/2017

Toward a better quantification of magnitudes of past stresses and fluid (over)pressures in sedimentary basins: insights from calcite twinning and stylolite roughness paleopiezometry

Olivier LACOMBE

UPMC SORBONNE UNIVERSITÉS

CNRS

Institut des Sciences de la Terre de Paris ISTeP SORBONNE UNIVERSITÉS

Why to characterize stresses in the crust ?

The motivation arises :

from applied geological purposes, such as geological hazards, engineering activities and resource exploration;

and

from fundamental geological purposes, such as understanding the mechanical behaviour of geological materials and deciphering various tectonic mechanisms, from those related to plate motions at a large scale to those causing jointing and faulting or even microstructures at a smaller scale.

Despite an increasing number of in situ stress measurements, magnitudes of crustal stresses remain poorly constrained…

Twinning of minerals depends on the magnitude of the applied shear stress.
One can make use of this property to evaluate the magnitude of the stress which has been supported by a rock during its history.

An access to paleostress magnitudes in the upper crust : Calcite twinning paleopiezometry

In the upper crust, brittle deformation of carbonate rocks is accompanied by pressure-solution, porosity reduction and crystalline deformation.

At low T (0-300°) calcite plasticity corresponds to the prevailance of e-twinning

How to constrain both orientations and magnitudes of past stresses (1) :

calcite twinning paleopiezometry

Twinning ~ simple shearing in a particular sense and direction along e-planes {01-12}

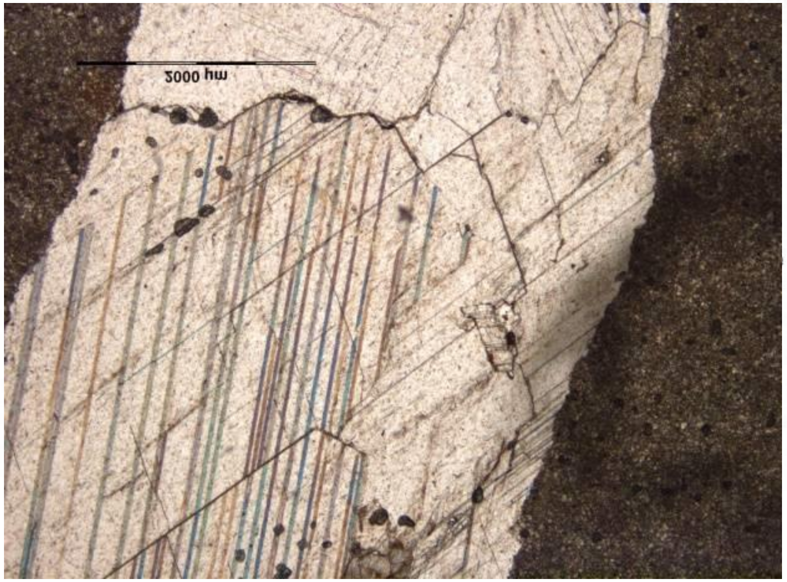

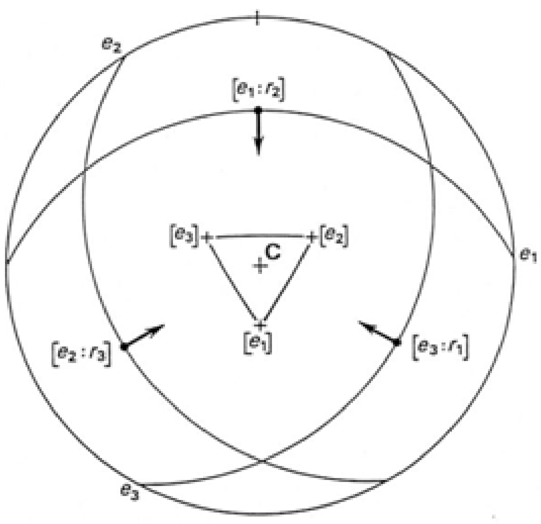

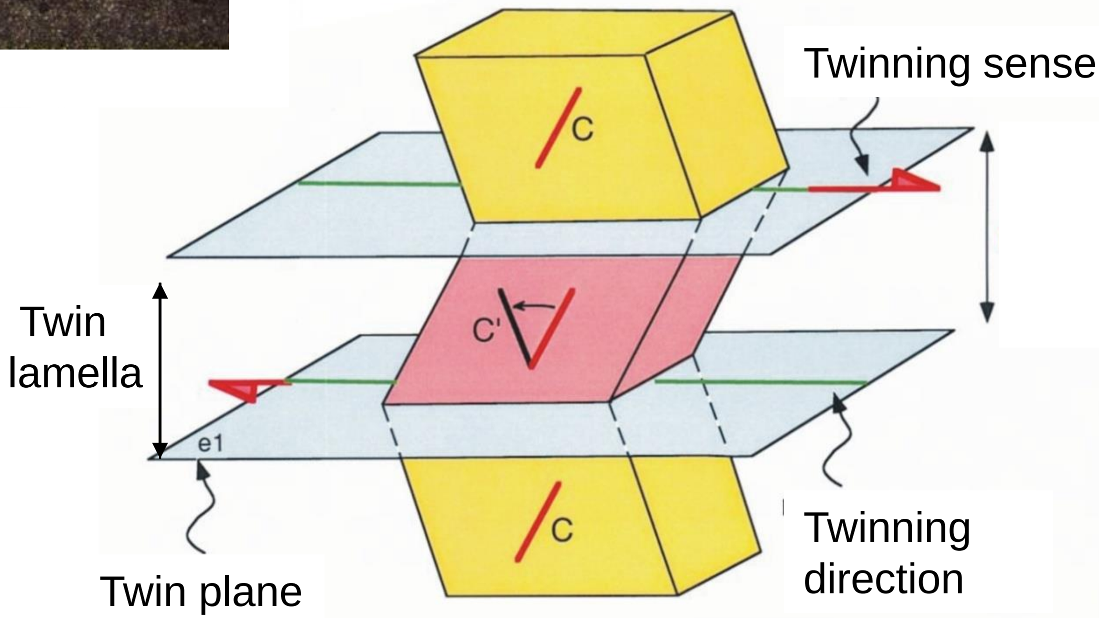

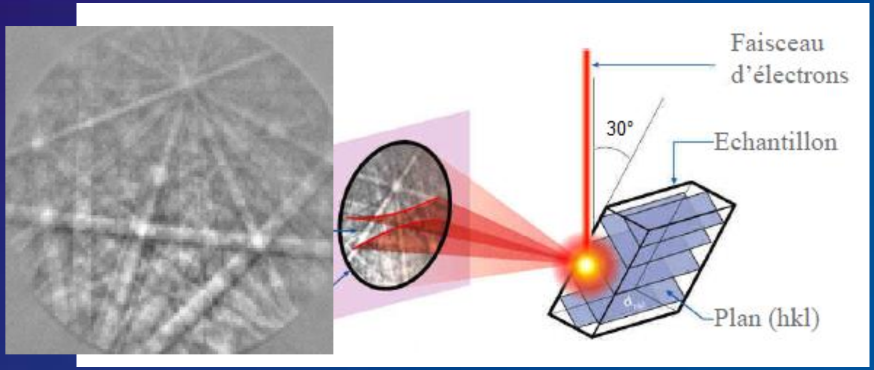

Measurement technique : U-stage /EBSD

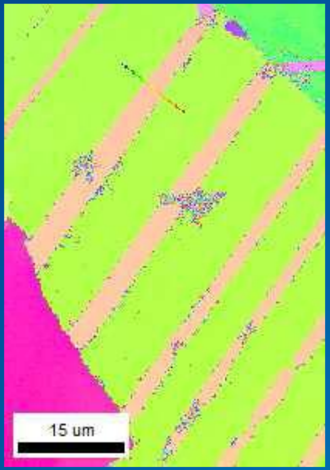

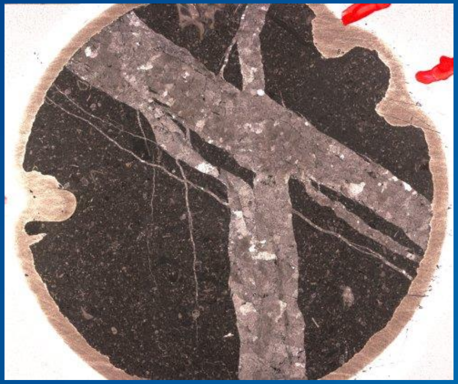

Material :
Host rock matrix / veins
Field samples or cores

Data : C-axis and twinned/untwinned planes in grains

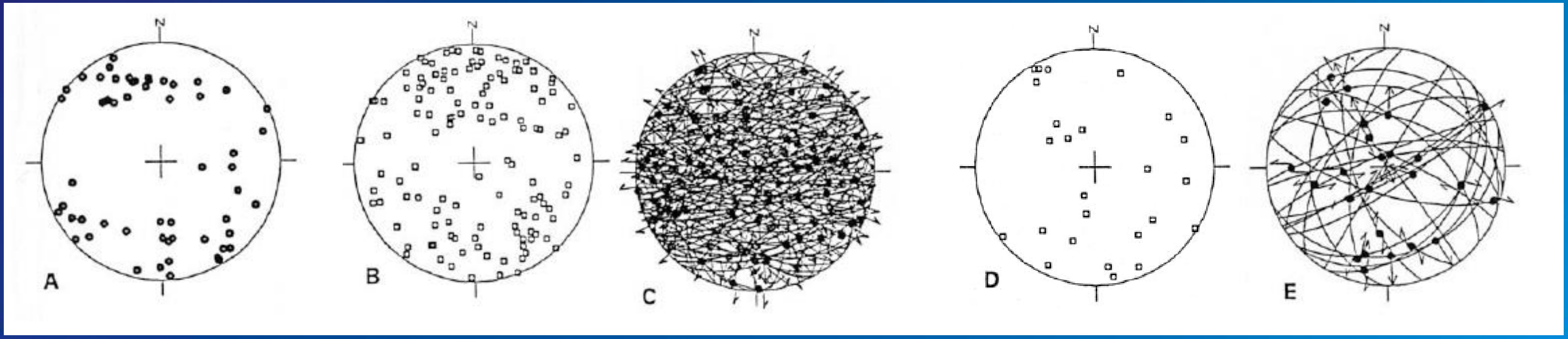

Stress analysis of calcite twinning :
The ‘historical’ techniques

Jamison and Spang (1976) :

determination of differential stress magnitudes

$$\tau_s = \Delta\sigma \cdot S$$

if τa is known, $\Delta\sigma$

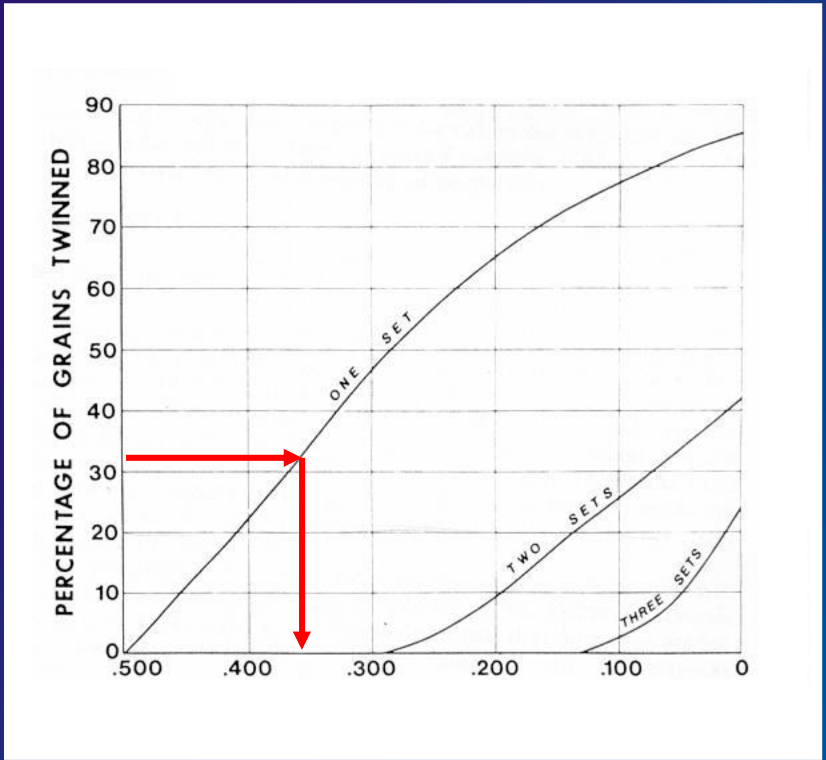

In a sample with no preferred crystallographic orientation, the percentages of grains twinned on 0, 1, 2 ou 3 twin planes are functions of the applied differential stress ($\sigma 1$-$\sigma 3$) value. Experimentally calibrated

Limitations :

- uniaxial stress
- critical resolved shear stress for twinning = constant τa = 10 MPa
- takes into account neither grain size nor mutual compatibility of twin systems

Rowe and Rutter (1990) : determination of differential stress magnitudes

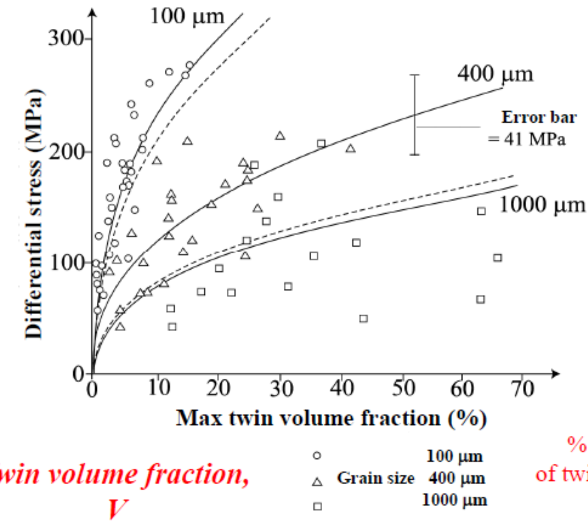

Twin volume fraction, V

% volume of twinned portion

$$\log \sigma = 2{,}72 + 0{,}40 \cdot (\log V - \log d)$$

Twin density, D

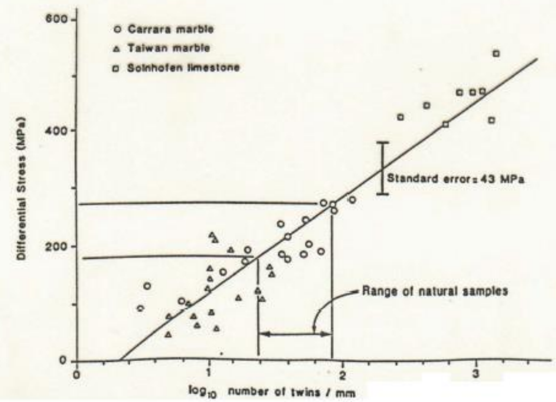

$$\sigma = -52{,}0 + 171{,}1 \,.\, \log D$$

Independant on grain size

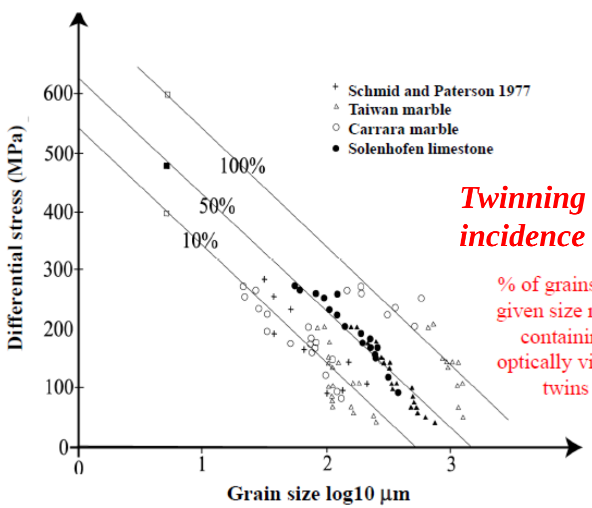

Twinning incidence

% of grains in a given size range containing optically visible twins

$$\sigma = 523 + 2{,}13\, It - 204 \cdot \log d$$

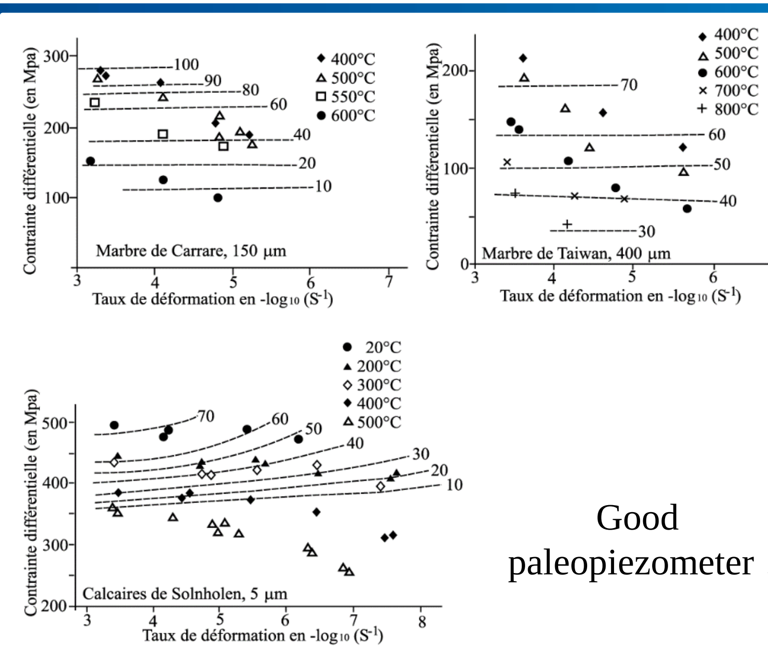

Good paleopiezometer !

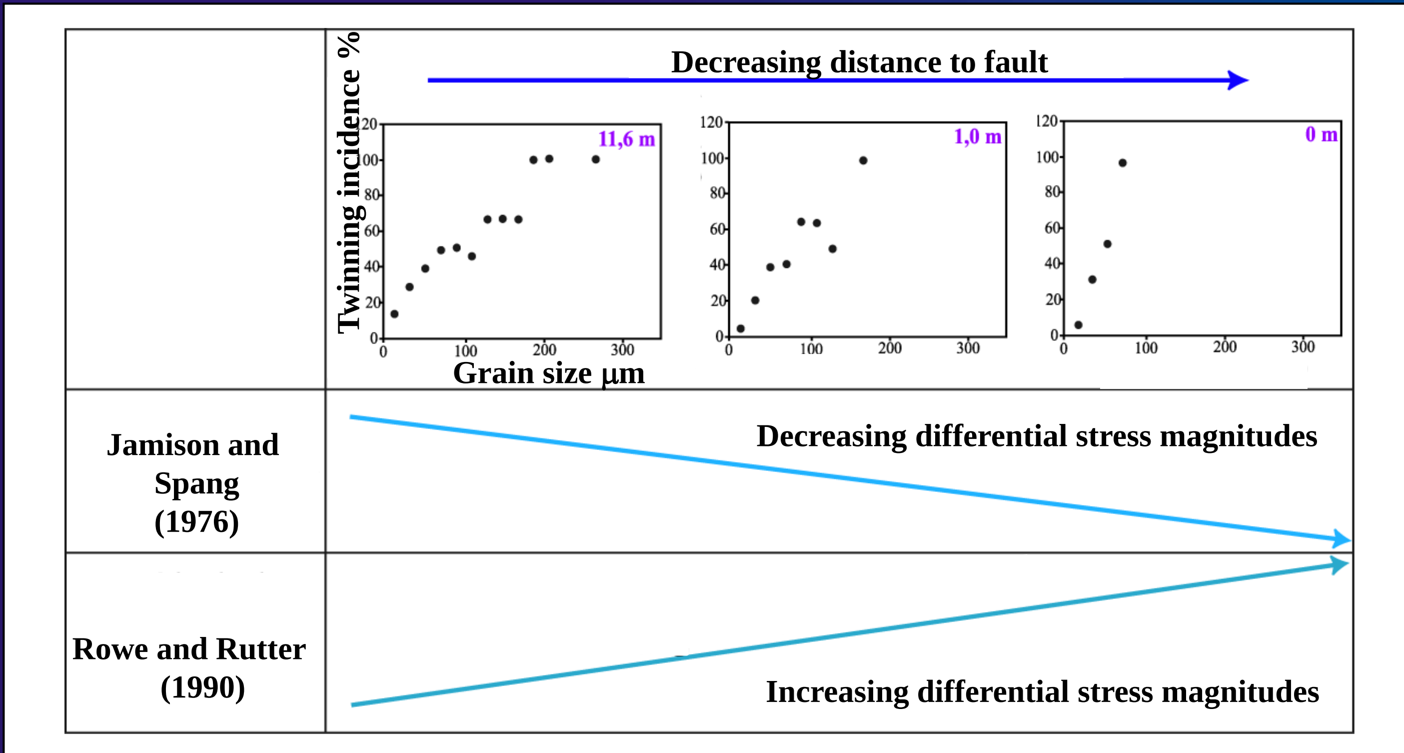

Influence of grain size distribution on estimates of differential stress magnitudes (Newman, 1994)

Région étudiée	Référence	Technique	Contraintes différentielles moyennes	Température de déformation
Nord de la chaine subalpine	Ferrill (1998)	Jamison et Spang (1976)	44 MPa	75 - 250 °C
		densité de macle de Rowe et Rutter (1990)	235 MPa	
Sud des Pyrénées	Holl & Anastasio (1995)	Jamison et Spang (1976)	65 MPa	190 - 235 °C
		densité de macle de Rowe et Rutter (1990)	249 MPa	

Influence of temperature on estimates of differential stress magnitudes (Ferrill, 1998)

Rowe and Rutter technique : well calibrated for T> 400°C, BUT cannot be used at low T

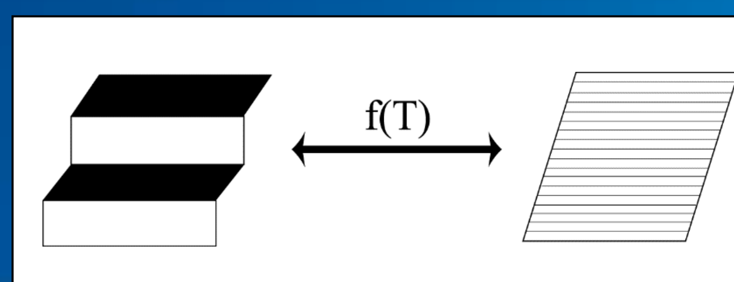

To sum up :

None of these techniques allows to relate differential stresses to principal stress orientations and stress regimes.

→ significance of ‘bulk’ maximum differential stresses in case of polyphase tectonics ?

Moreover,
techniques are commonly used separately without care of their specific limitations

The Calcite Stress Inversion Technique CSIT 1/2

(Etchecopar, 1984; Parlangeau et al., 2018)

Determination of the reduced stress tensor

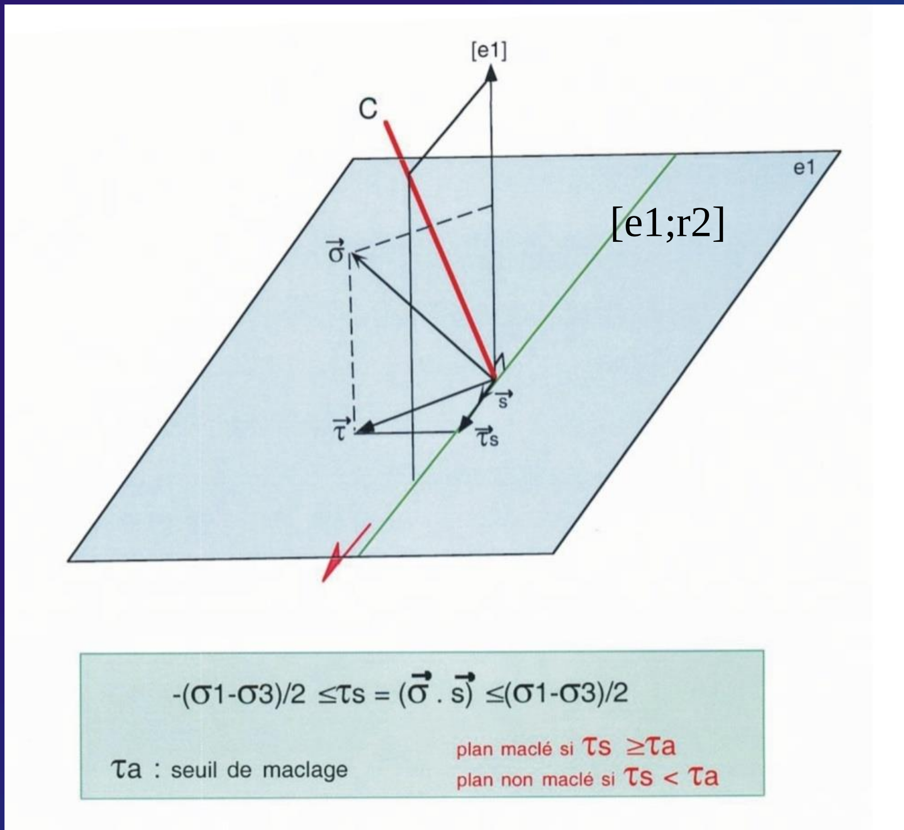

Inversion of calcite twin data ⇨ **Reduced stress tensor (4 parameters)**

Orientation of principal stresses and stress ratio

$$\Phi = \frac{(\sigma_2 - \sigma_3)}{(\sigma_1 - \sigma_3)}$$

+ dimensionless differential stress $(\sigma_1 - \sigma_3)/\tau a$

<u>The inversion process is very similar to that used for fault-slip data</u> : twin gliding along the twinning direction within the twin plane is geometrically is comparable to slip along a slickenside lineation within a fault plane.

But the inversion process takes into account both twinned planes (resolved shear stress > CRSS)

<u>**AND**</u>

untwinned planes (resolved shear stress < CRSS), <u>a major difference with inversion of fault-slip data</u>

Critical Resolved Shear Stress (CRSS) τa = resolved shear stress along the twinning direction that must be reached to induce a significant plastic (permanent) deformation, i.e., to induce motion of a number of dislocations so that sliding becomes macroscopically observable.

Commonly associated with a critical point on the stress-strain curve for a monocrystal.

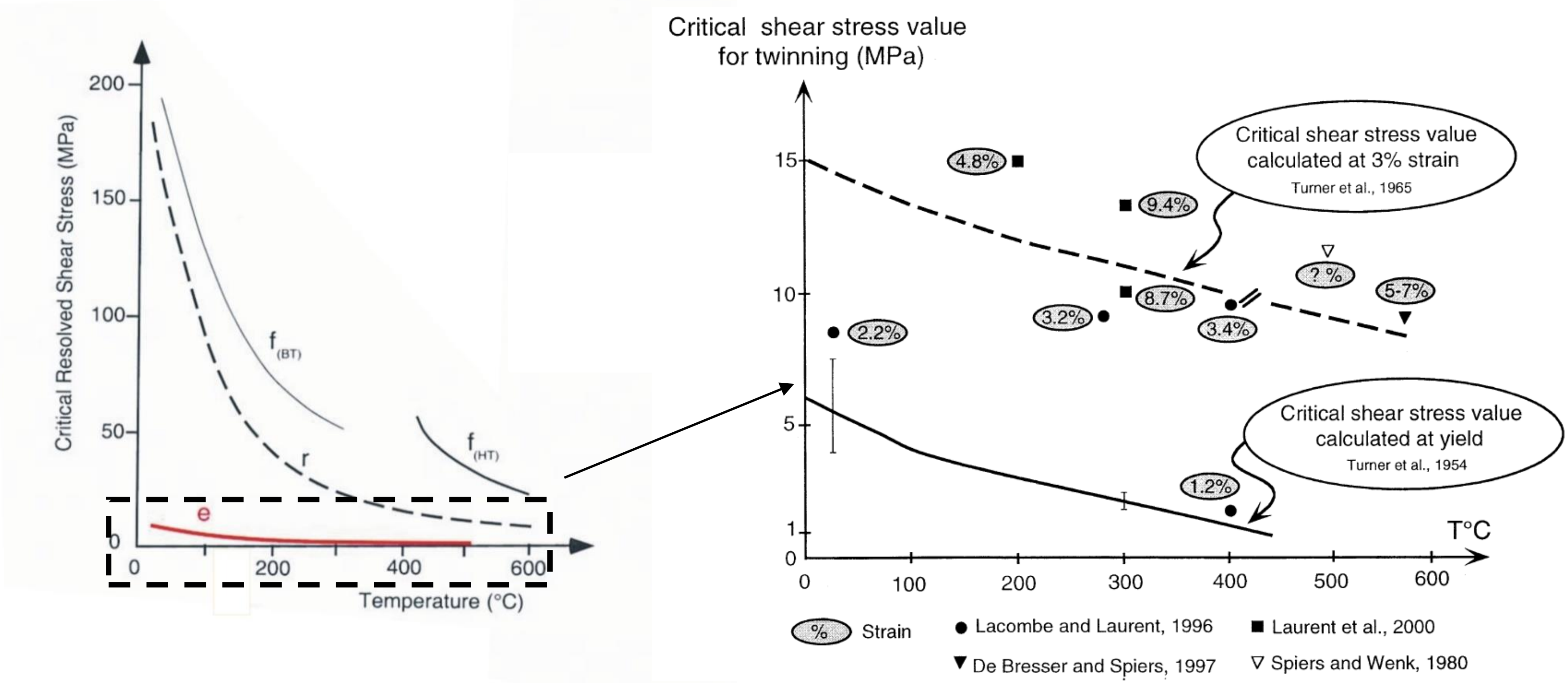

(Lacombe, 2001, 2010)

The CRSS is ~ independent on T°C but depends on grain size and internal strain (hardening)

Inversion of calcite twin data → **Reduced stress tensor (4 parameters)**

Orientation of principal stresses and stress ratio

$$\Phi = \frac{(\sigma_2 - \sigma_3)}{(\sigma_1 - \sigma_3)}$$

+ dimensionless differential stress

$$(\sigma_1 - \sigma_3) / \tau a$$

'constant' CRSS τa
for a set of calcite grains
of homogeneous size

Deviatoric stress tensor (5 parameters)

$$T_D = T - \left(\frac{\sigma_1 + \sigma_2 + \sigma_3}{3} \right) \cdot I$$

Orientation of principal stresses and differential stress magnitudes

$$(\sigma_1 - \sigma_3) \quad (\sigma_2 - \sigma_3)$$

Some applications of calcite twin analysis for reconstructing regional tectonic evolution

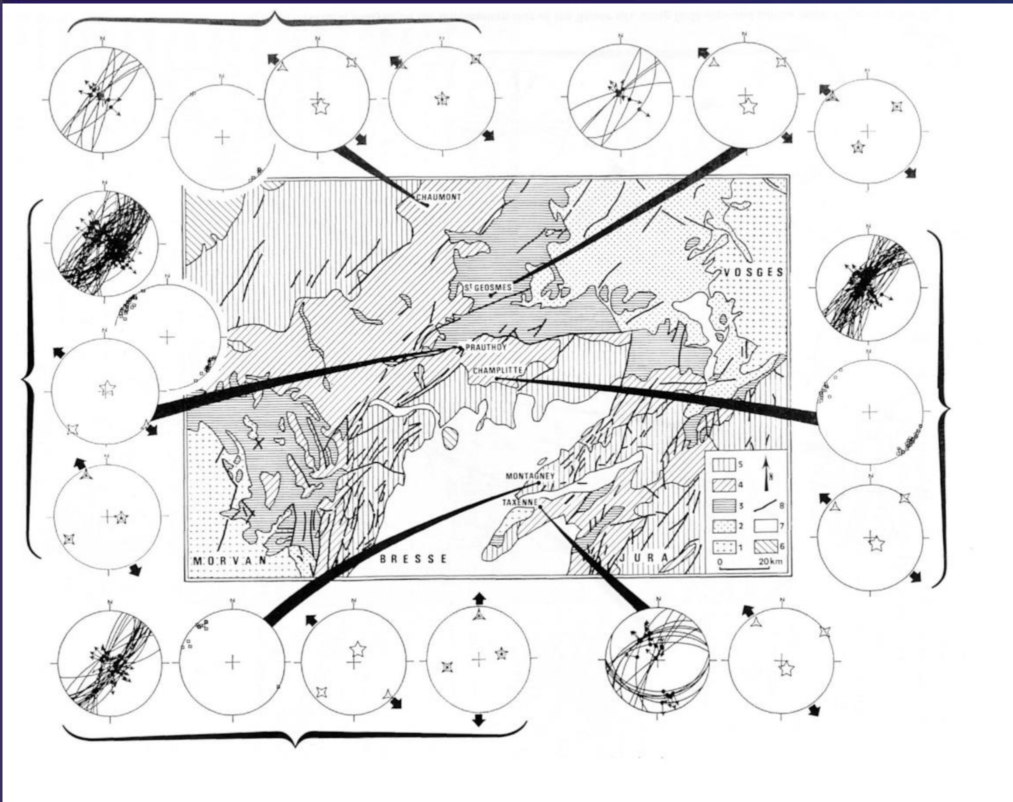

Provence, Eocene compression
(Lacombe et al., 1991)

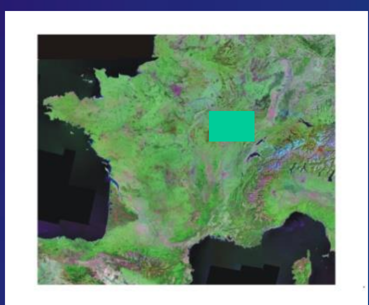

Burgundy, Oligocene extension
(Lacombe et al., 1990)

Consistency between calcite twin data and fault-slip data in term of regional paleostress record

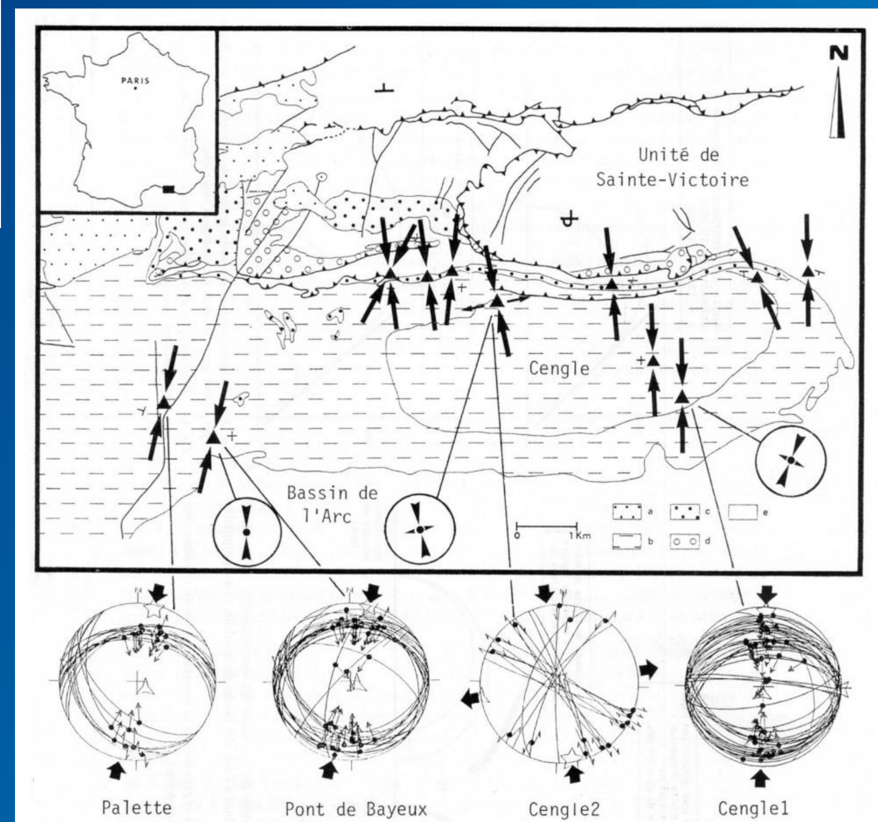

Zagros : Neogene/ongoing collision between Arabia and Central Iran

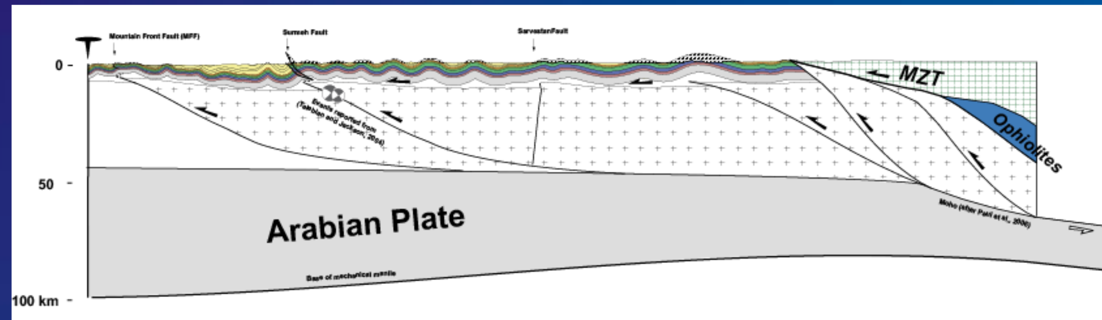

Collisional stresses consistently recorded at all scales

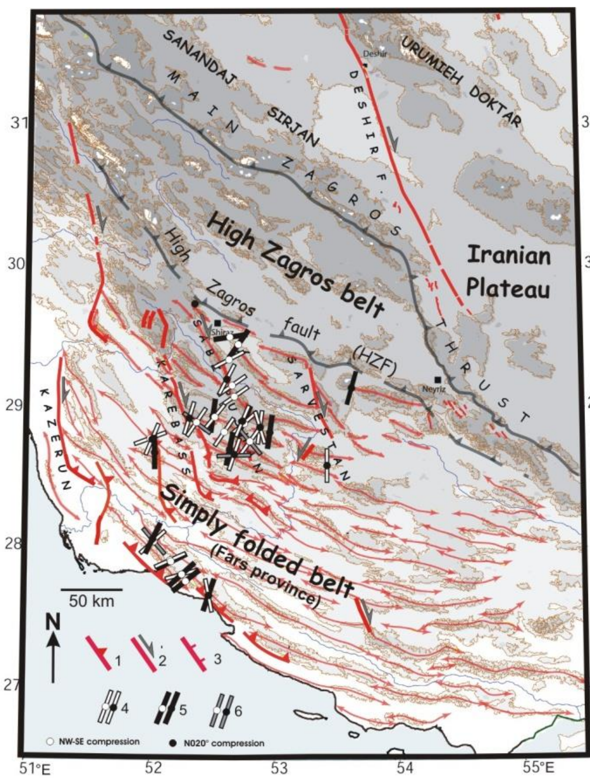

Neogene compressional trends from fault slip data (Lacombe et al., 2006)

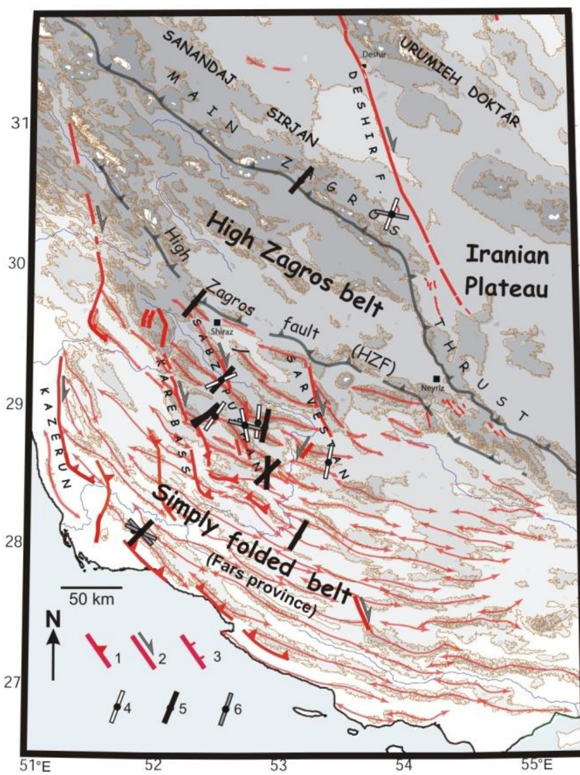

Neogene compressional trends from calcite twin data (Lacombe et al., 2007)

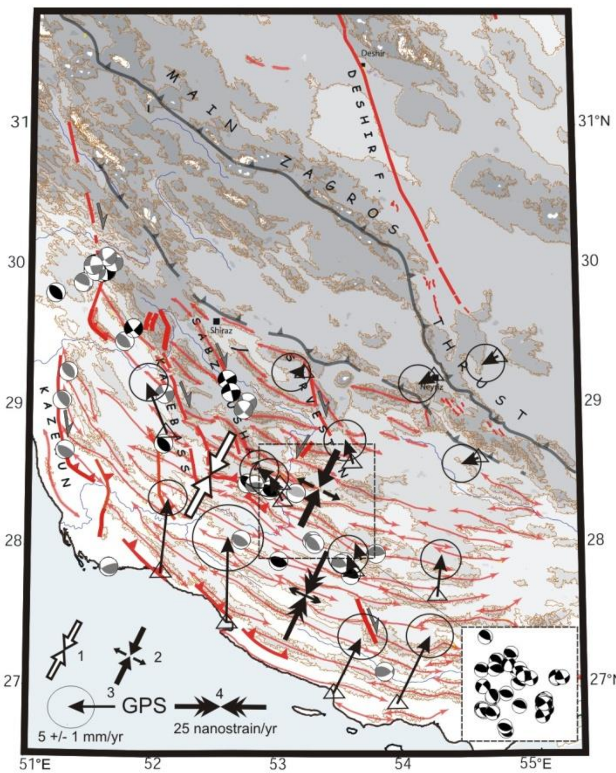

Current compressional trends from earthquake focal mechanisms (Lacombe et al., 2006) and GPS shortening rates (Walpersdorf et al., 2006)

Differential stress magnitudes
in fold-and-thrust belts and orogenic forelands

(Lacombe et al., 2007)

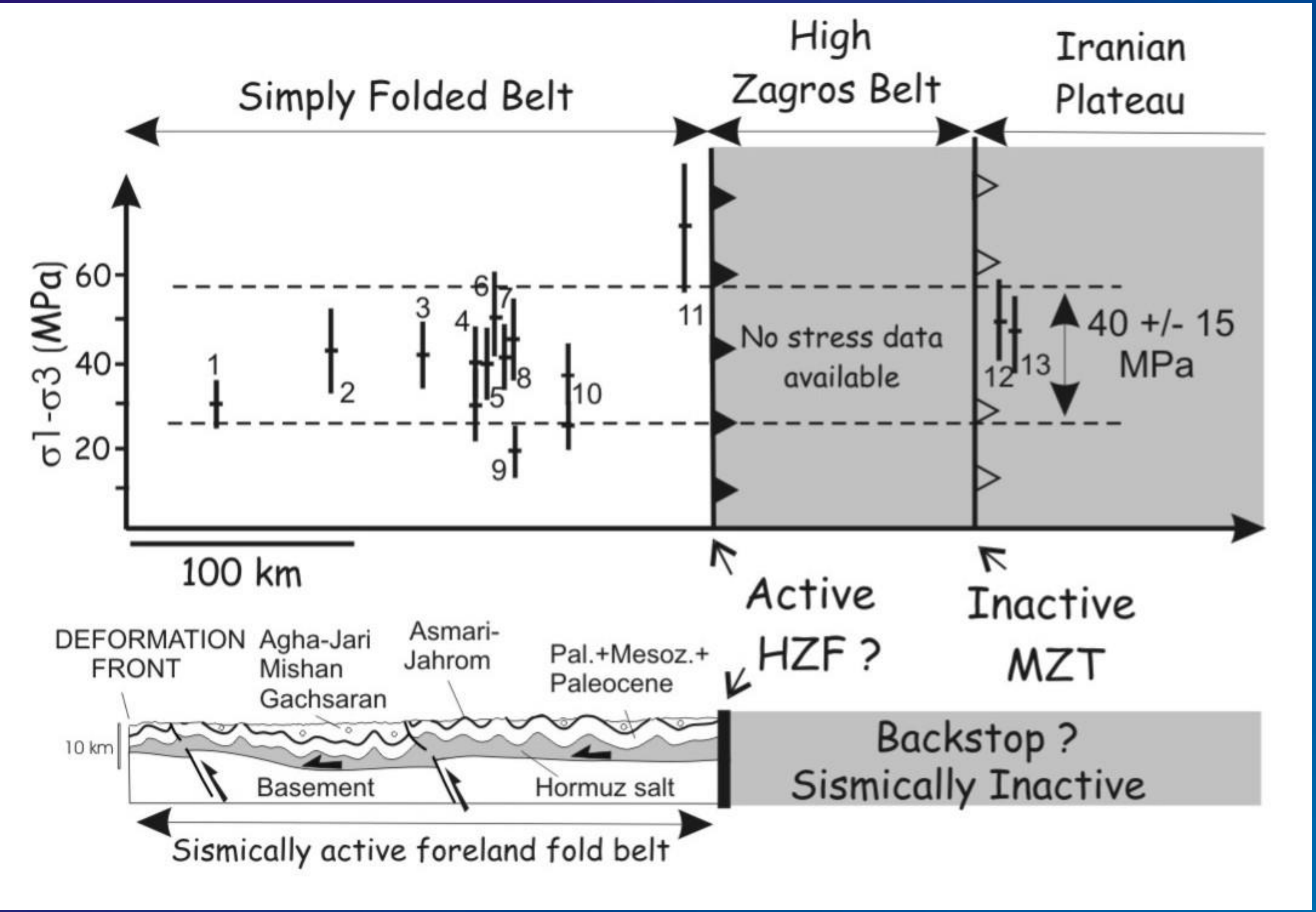

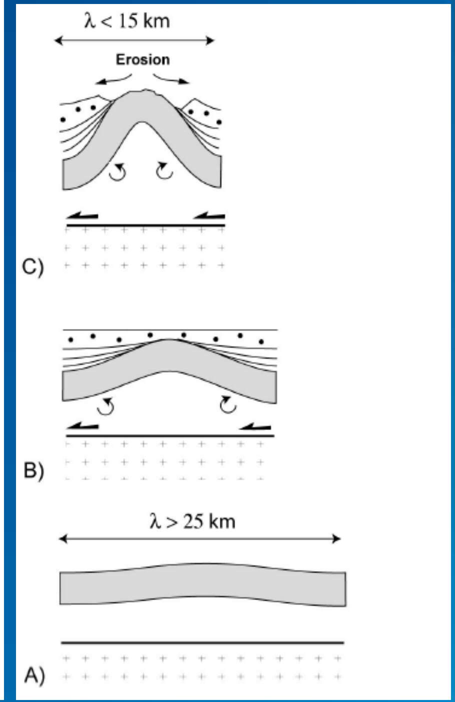

The relative homogeneity of differential stresses agrees with the homogeneously distributed shortening across the SFB, where no deformation gradient toward the backstop is observed in contrast to classical fold-thrust wedges

Both pre- and post-folding differential stresses are low --> folding likely occurred at low stresses; this favours pure-shear deformation and buckling of sedimentary rocks rather than brittle tectonic wedging.

(Hnat et al., 2013;
Van der Pluijm et al., 1997)

(Lacombe et al., 2007)

(Xypolias & Koukouvelas, 2005)

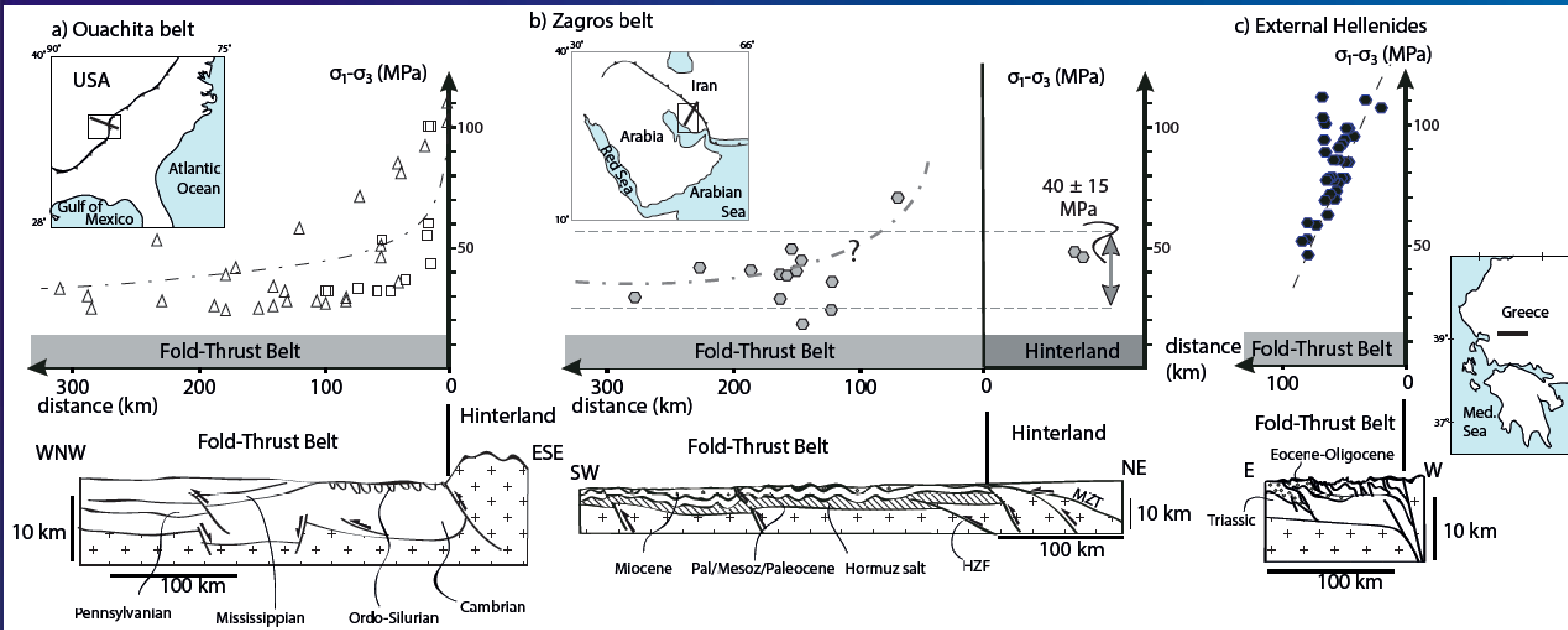

(Beaudoin and Lacombe, submitted)

… and also in the north Pyrenean foreland
(Lacombe et al., 1996; Rocher et al., 2000)…

Paleo-differential stress vs paleodepth

On the difficulty of establishing a paleostress/ paleodepth relationship

In drill holes, contemporary stresses are determined directly at a given depth / in a narrow depth interval.

In contrast, paleopiezometers are generally sampled and analysed after they have reached the surface, i.e., after exhumation from an unknown depth z, and establishing a $\Delta\sigma$ vs z relationship for paleostresses requires independent determination of $\Delta\sigma$ and z.

In FTBs, paleo-z estimates are usually derived from stratigraphic/ sedimentological studies or from thermometry coupled with assumption on paleothermal gradient

In addition, in case of polyphase tectonism, deciphering the $\Delta\sigma$ vs z evolution requires to unambiguously relate $\Delta\sigma$ to both z and to a specific tectonic event.

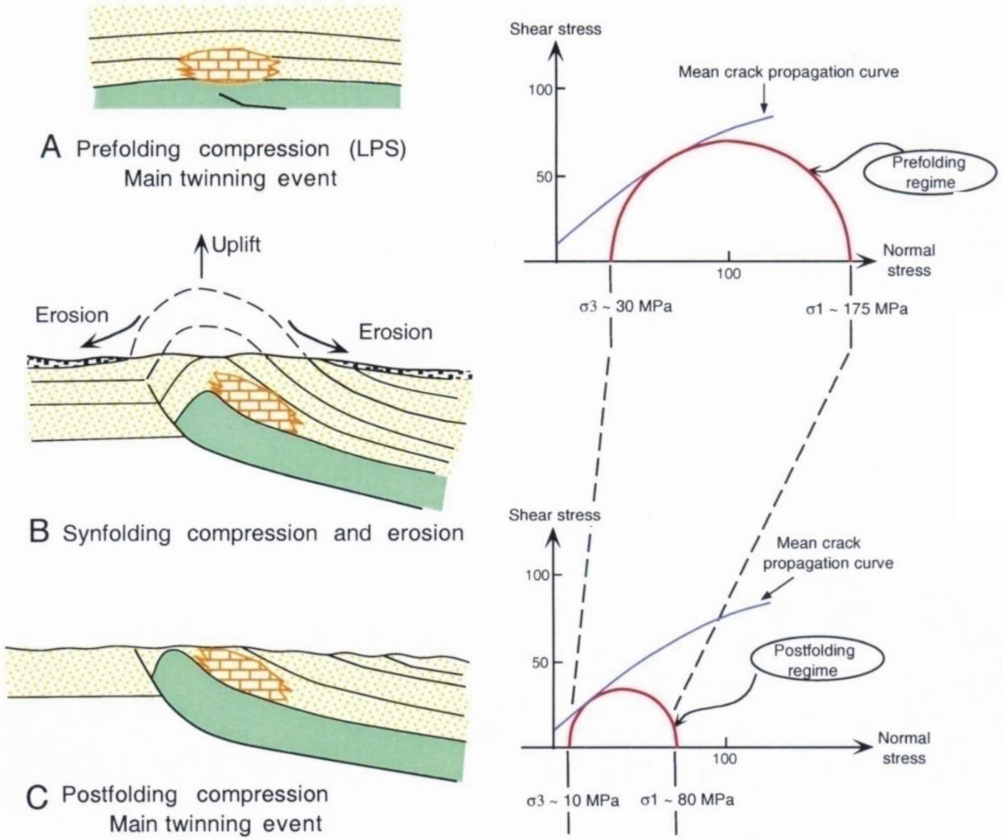

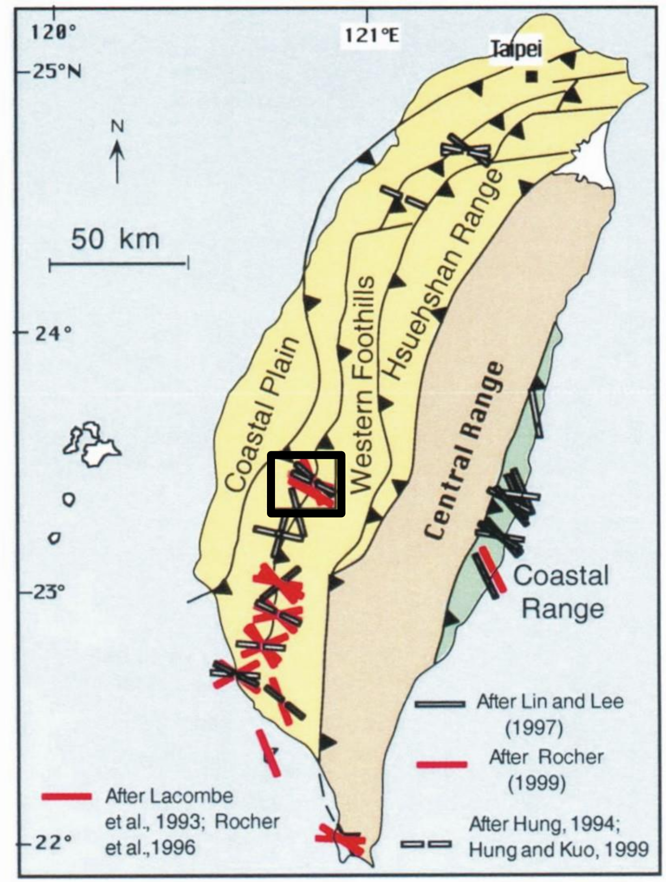

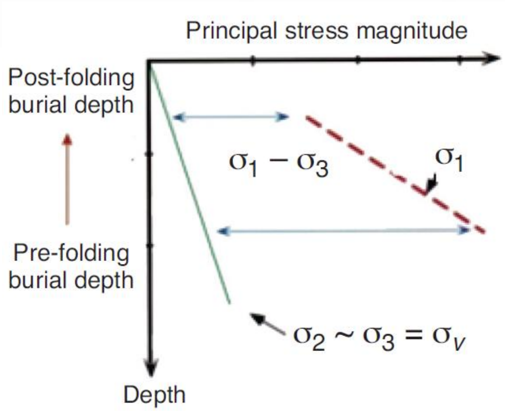

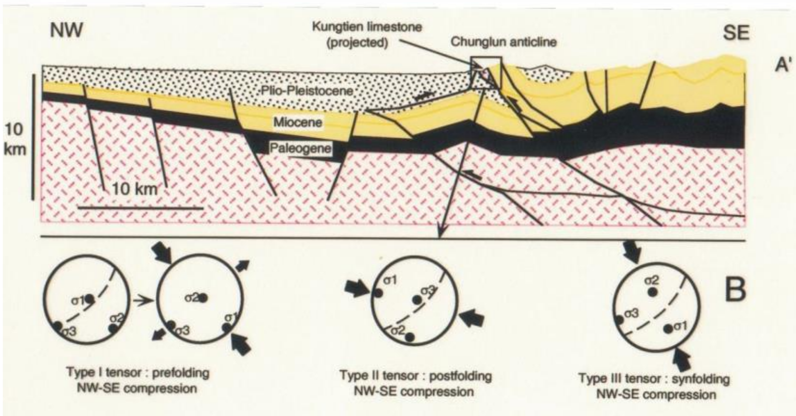

(Lacombe, 2001)

For a favourably oriented pre-existing cohesionless fault plane, the condition of reactivation can be written as follows :

$$(\sigma_1 - P_f)/(\sigma_3 - P_f) = [(\mu^2 + 1)^{0.5} + \mu]^2$$

$$\sigma_1 - \sigma_3 = 2\rho g z(\lambda - 1)(1 - [(\mu^2 + 1)^{0.5} + \mu]^2) / (1 + [(\mu^2 + 1)^{0.5} + \mu]^2)$$

Strike-slip stress regime

and

Reverse stress regime

$$\sigma_1 - \sigma_3 = \rho g z(\lambda - 1)(1 - [(\mu^2 + 1)^{0.5} + \mu]^2)$$

with $\lambda = P_f/\rho g z$

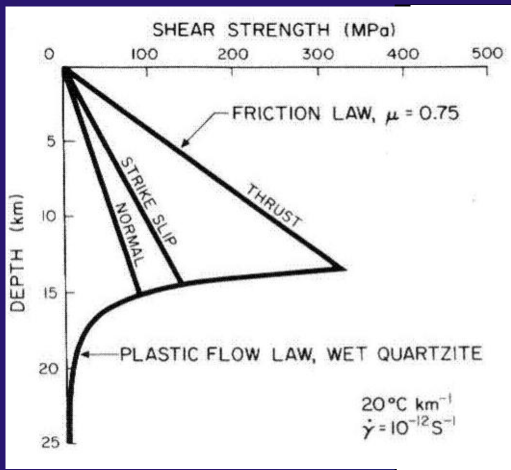

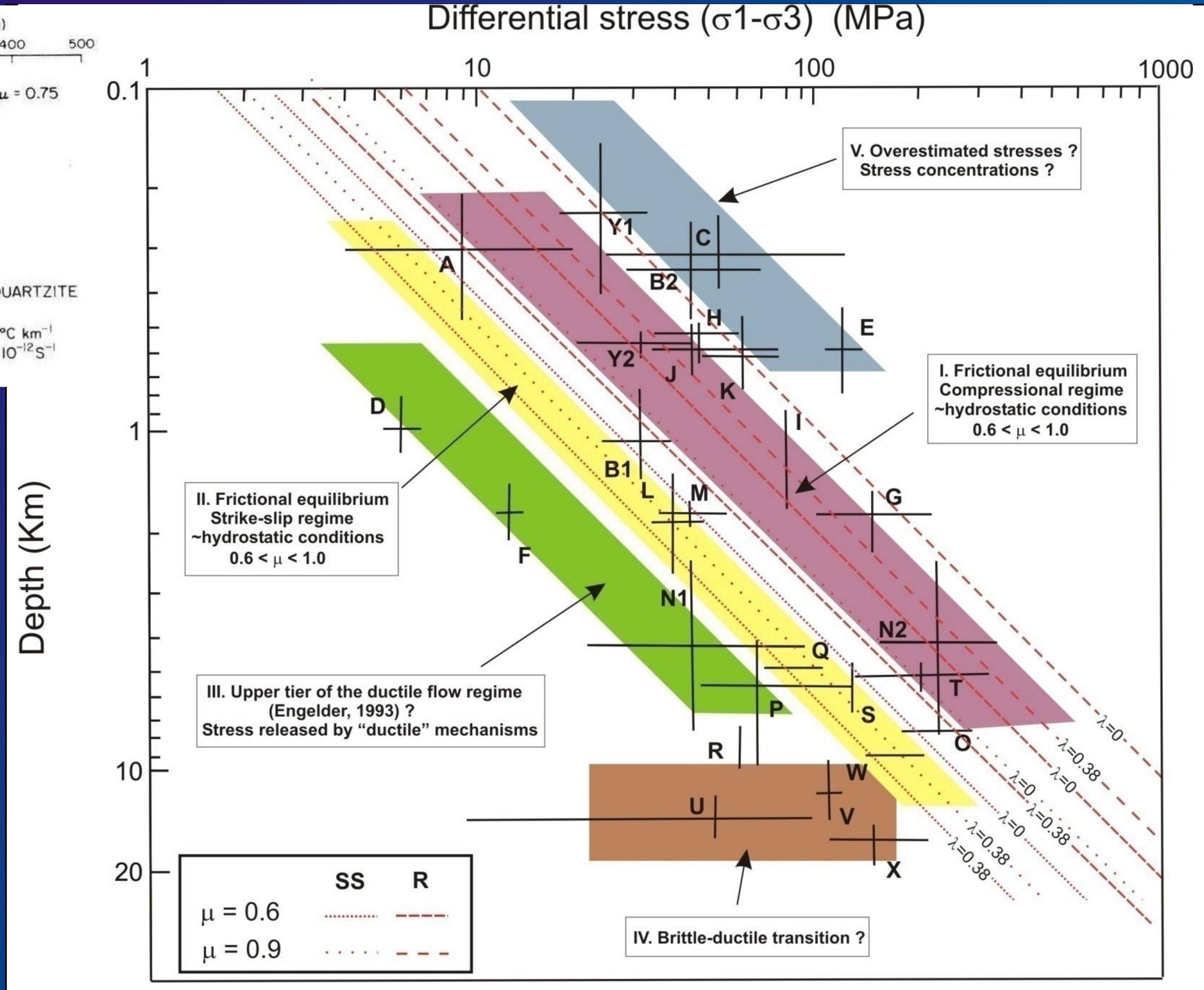

(Lacombe, 2007)

Most paleostress data support a first-order frictional behaviour of the upper continental crust.

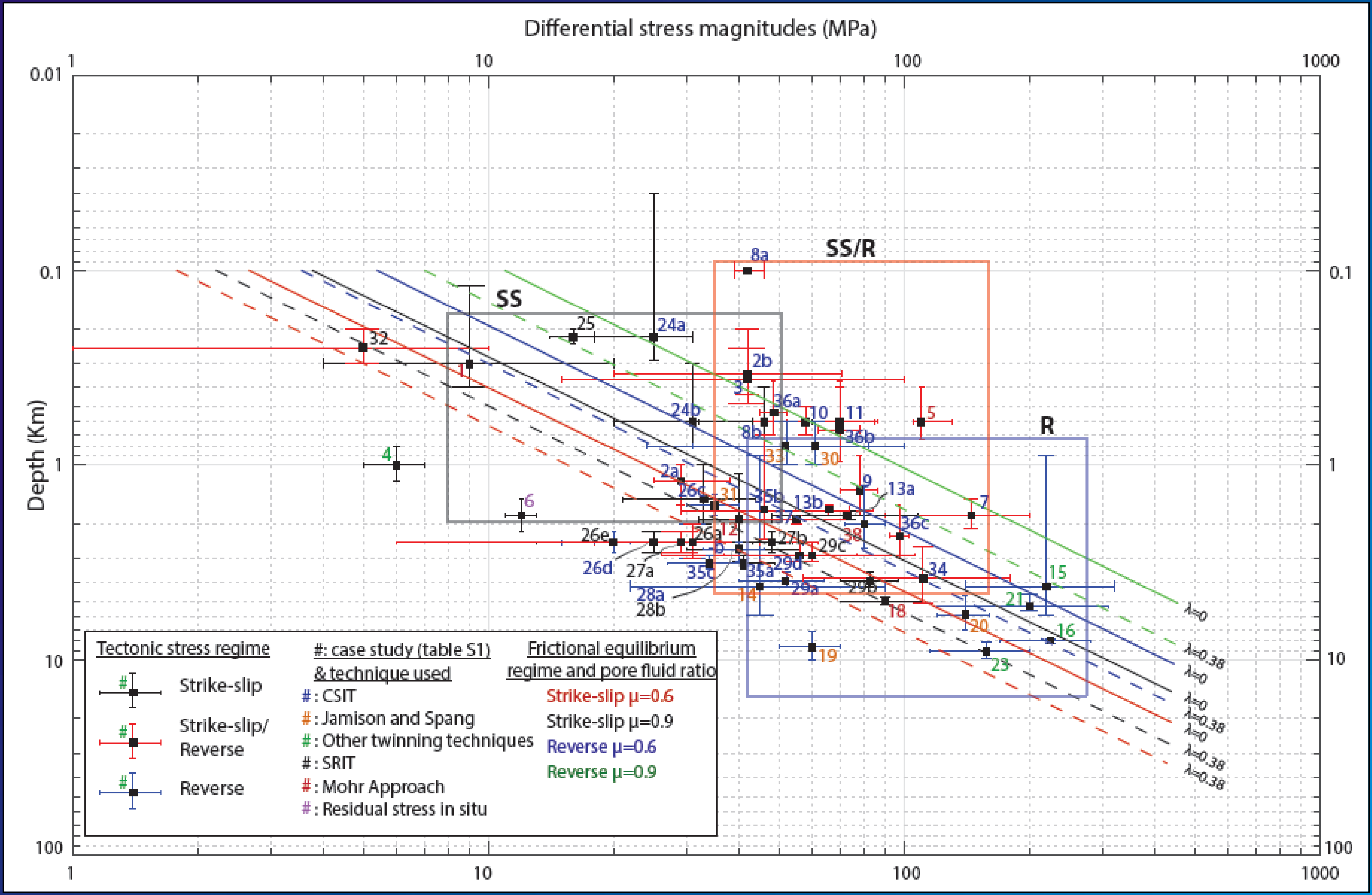

(Beaudoin and Lacombe, submitted)

At the present-day state of our knowledge and with the available dataset, most paleostress data support a first-order long-term frictional behaviour of the upper continental crust.

The crustal strength down to the brittle-ductile transition is generally controlled by frictional sliding on well-oriented pre-existing faults with frictional coefficients of 0.6-0.9 under hydrostatic fluid pressure (frictional stress equilibrium).

Some ductile mechanisms may, however, relieve stress and keep stress level beyond the frictional yield, as for instance in the detached cover of forelands.

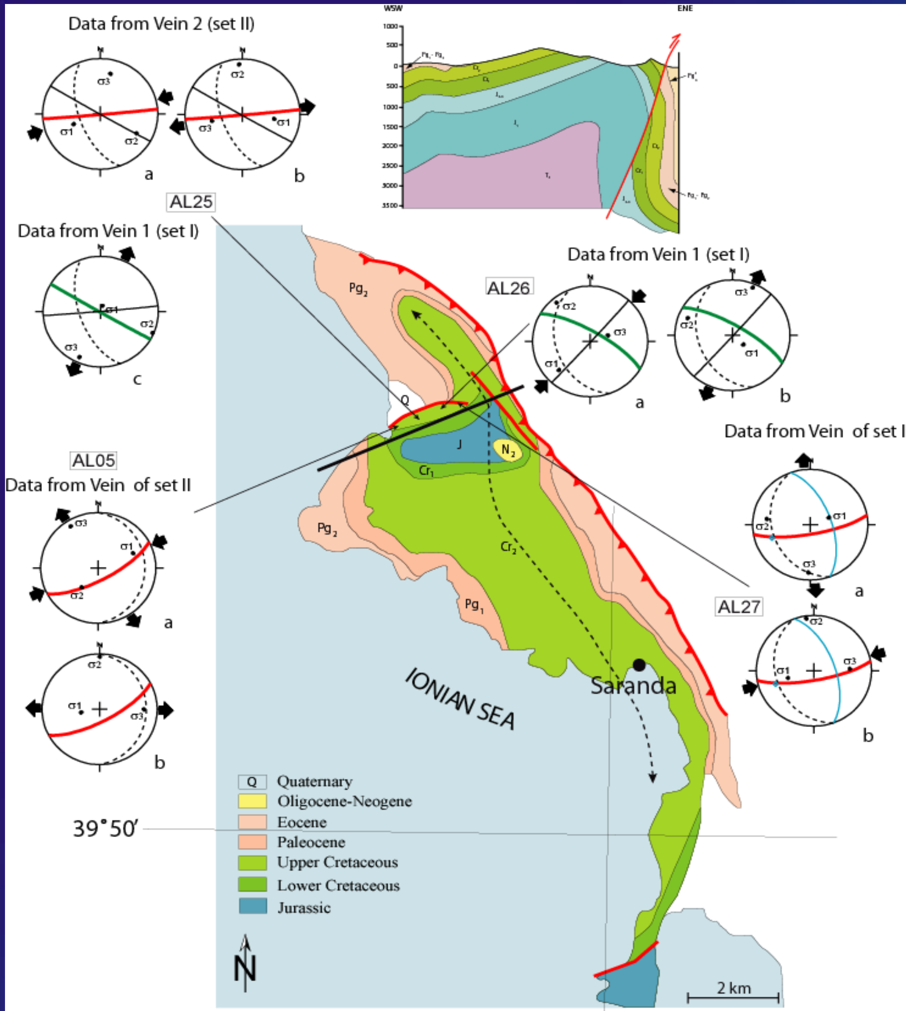

(Lacombe et al., 2009)

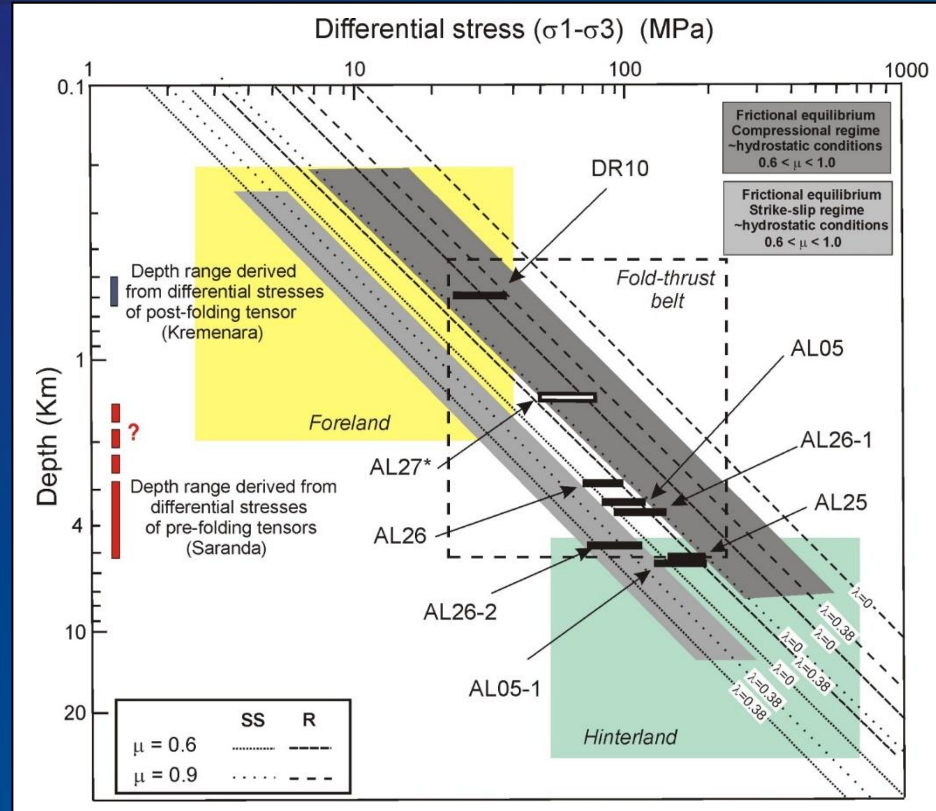

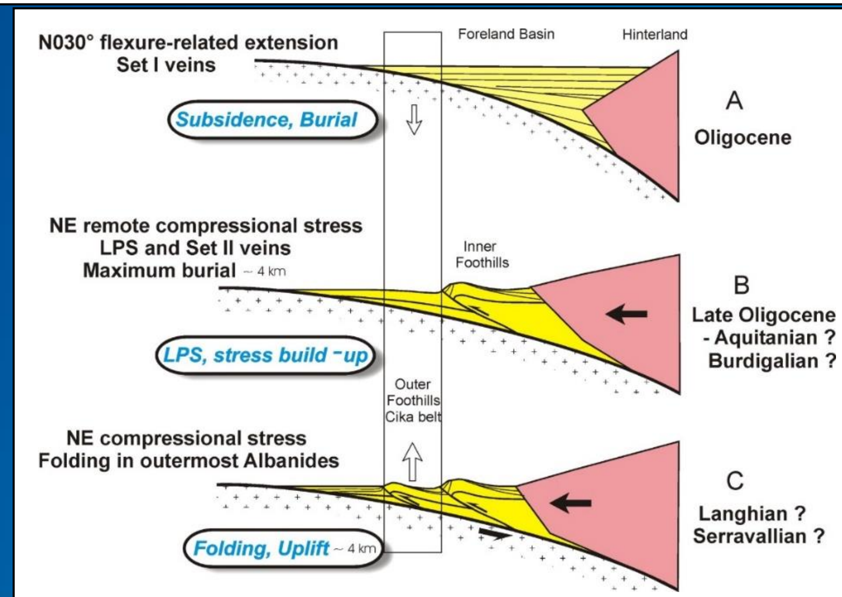

Calcite twins provide estimates of pre-folding paleoburial consistent with independent estimates from micro-thermometry of fluid inclusions, maturity of organic matter and results of 1D thermal modeling.

How to constrain both orientations and magnitudes of past stresses (2) :

Stylolite roughness paleopiezometry

Thermodynamics and kinetics of the growth of a stylolite :

Once dissolution starts, there is a competition between:

- two stabilizing (smoothening) forces, long-range elastic forces and local surface tension, that tend to reduce the Helmholtz free energy of the solid → they flatten the surface by preferentially dissolving areas of local roughness ;

- a destabilizing (roughening) force due to pinning particles on the stylolitic surface, that resists dissolution in specific locations, locally increasing the free energy and producing peaks and teeth.

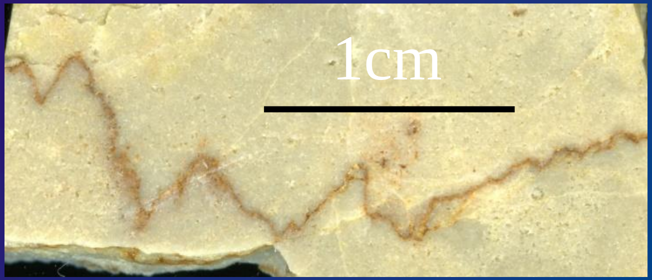

.

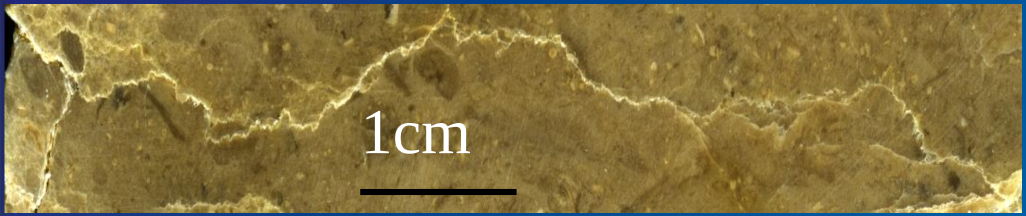

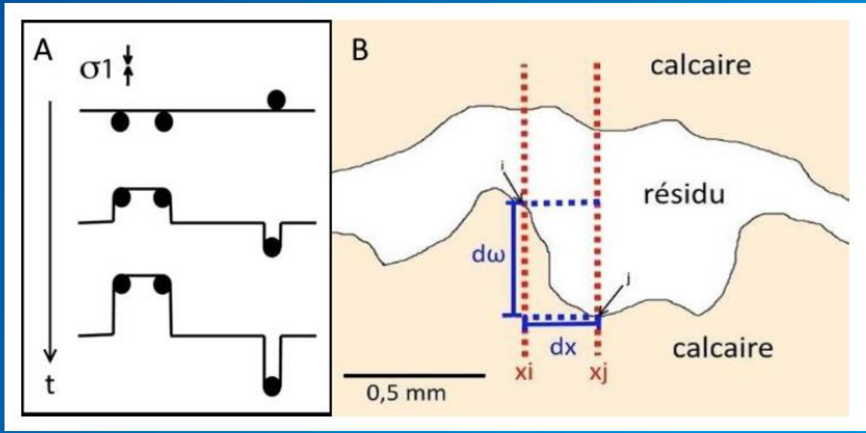

scaling of the roughness

Fourier Power Spectrum

$$P(k) = k^{D-2h}$$

if the signal is self-affine

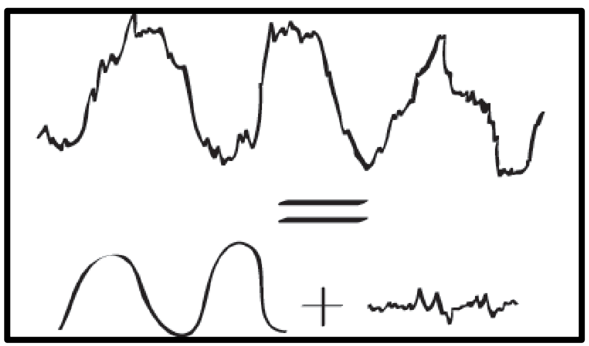

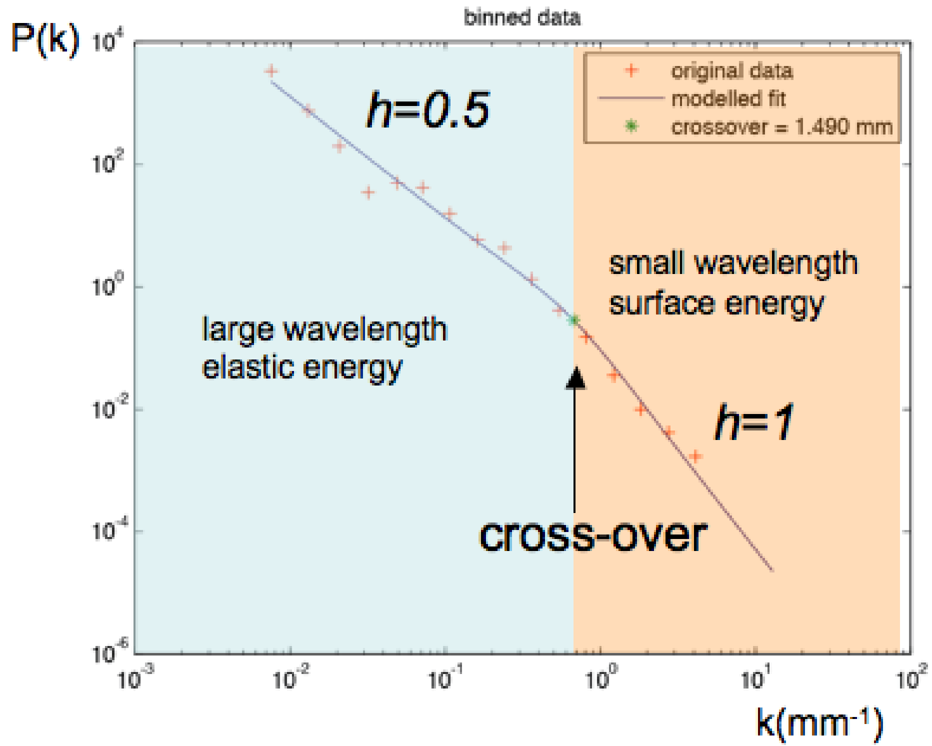

→ two growth regimes (elastic / surface energy dominated regimes), each of those being characterized by a roughness exponent (Hurst exponent) and separated by a crossover length (Lc) that describes the scale at which the switch between regimes of control occurs.

(Schmittbuhl et al., 2004)

$$L_c = \frac{\gamma E}{\beta \sigma_m \sigma_d}$$

γ : surface energy at the solid-fluid interface, E : Young modulus,
$\beta = \nu(12\nu)/\pi$: dimensionless number with ν : Poisson ratio,
σm : mean stress, σd : differential stress.

Considering an isotropic stress in the stylolite plane
(sedimentary/bedding-parallel stylolites - BPS) :

$$\left| \begin{array}{l} \sigma_v > \sigma_H = \sigma_h \\ \sigma_H = \sigma_h = \left(\frac{\nu}{1-\nu}\right) \sigma_v \end{array} \right. \rightarrow \left| \begin{array}{l} L_c = \dfrac{\gamma E}{\beta \alpha \sigma_v{}^2} \\ \alpha = \frac{1}{3} \left(\frac{1+\nu}{1-\nu}\right) \left(\frac{1-2\nu}{1-\nu}\right) \end{array} \right. \rightarrow \left| \begin{array}{l} \sigma_v = \sqrt{\dfrac{\gamma E}{L_c \beta \alpha}} \\ \sigma_H = \sigma_h = \left(\frac{\nu}{1-\nu}\right) \sigma_v \end{array} \right.$$

This allows to predict the magnitudes of the normal-to-the-plane stress
and of the two in-plane stresses

In contrast, a tectonic stylolite records a stress anisotropy within the stylolite plane (σ2 different from σ3) : depending on the orientation of the stylolite the crossover length Lc reflects the differential stress σ1-σ2, σ1-σ3 or a value in between.

If Lc is determined from a 2-D signal, then it depends on the orientation of the cut through the stylolite with respect to σ2 and σ3 (σ1 horizontal and normal to stylolite).

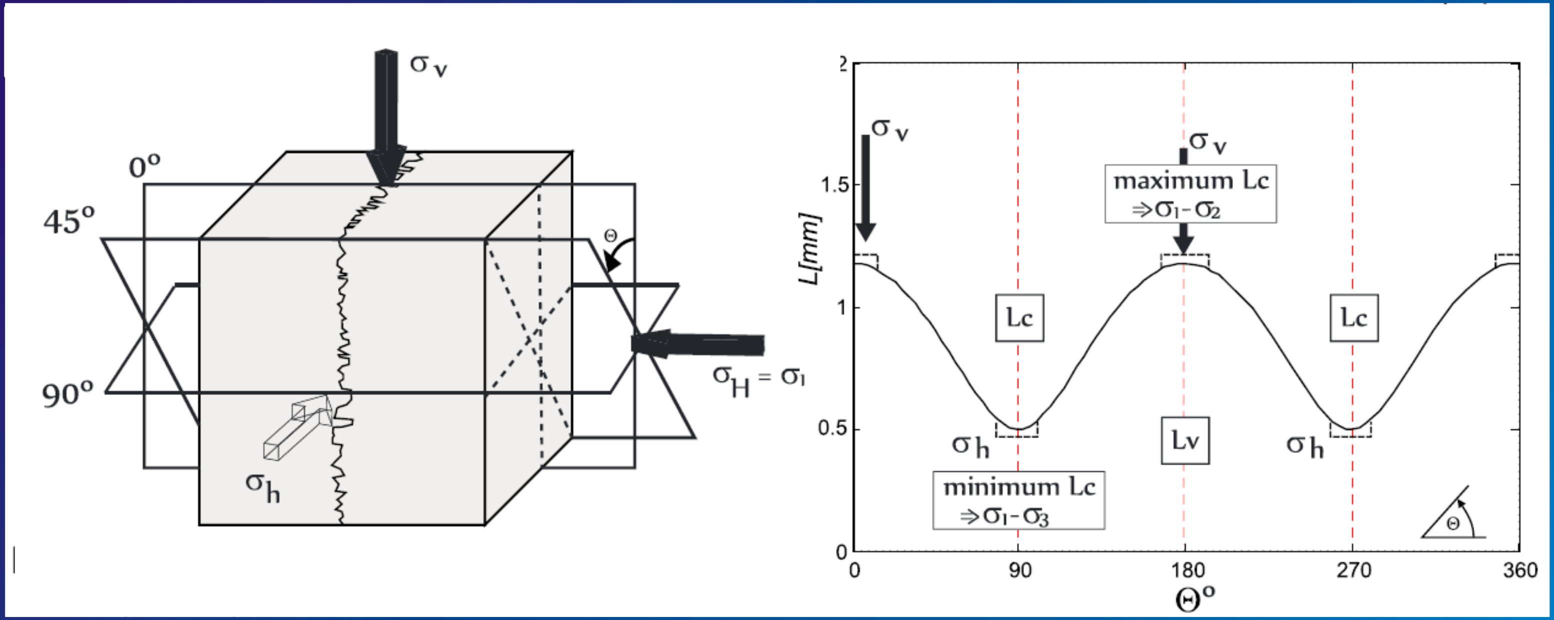

The relationship between Lc and the angle θ is a periodic function, with minimum and maximum Lc separated by 90° → roughness inversion on 2-D scans of three surfaces normal to the stylolite yields 3 Lc and the 3 corresponding angles θ between the cuts and the vertical direction.

The minimum and the maximum Lc correspond to (σ1-σ3) and (σ1-σ2). If θ associated with Lcmin is close to the vertical plane, then σ2 is vertical (SS regime); otherwise, if θ associated with Lcmax is close to 0°, then σ3 is vertical (R regime).

To summarize, Stylolite Roughness Inversion (SRI) works for :

- Stress direction
- Depth of sedimentary stylolites (from shallow to 4000m)
- Stress associated with tectonic stylolites (needs 3D and assumption of depth)

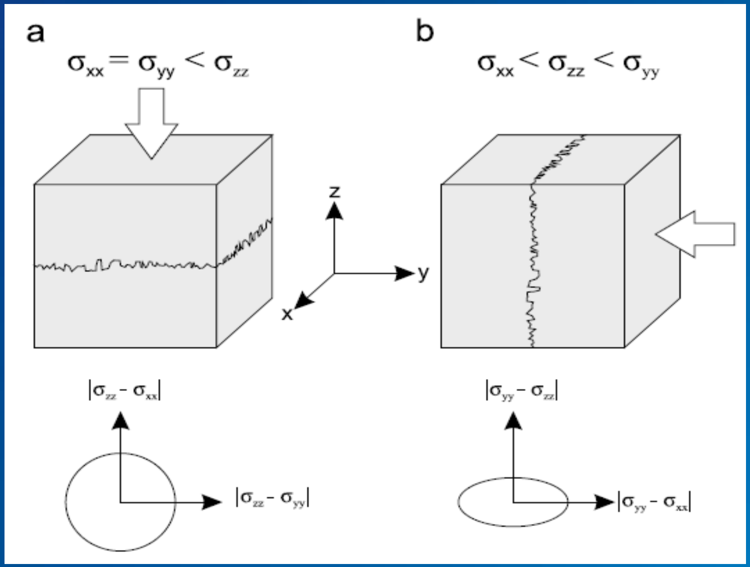

Sedimentary stylolites	Tectonic stylolites
$\sigma_z^2 = \frac{\gamma E}{\alpha\beta L_c}$	$\sigma_y = \mathrm{f}(\frac{L_v}{L_h}; \sigma_z) \pm \sqrt{\Delta(\frac{L_V}{L_h}, \sigma_z, \frac{a}{L_h})}$
$\sigma_x = \sigma_y = \frac{\nu}{1-\nu}\sigma_z$	$\sigma_x = \sigma_y - \frac{L_V}{L_h}\sigma_y - \frac{L_V}{L_h}\sigma_z$

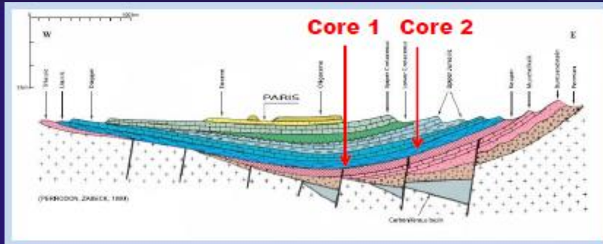

2 Jurassic cores (margin *versus* depocenter) were chosen.

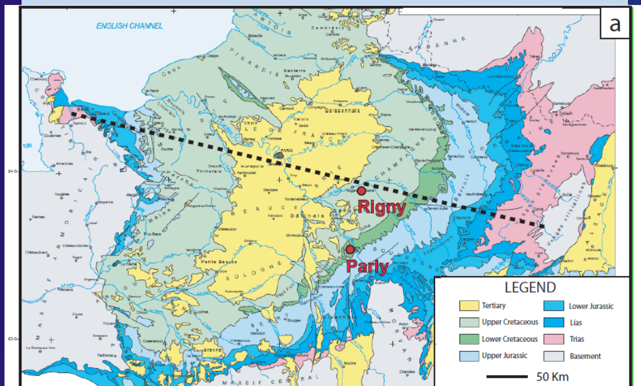

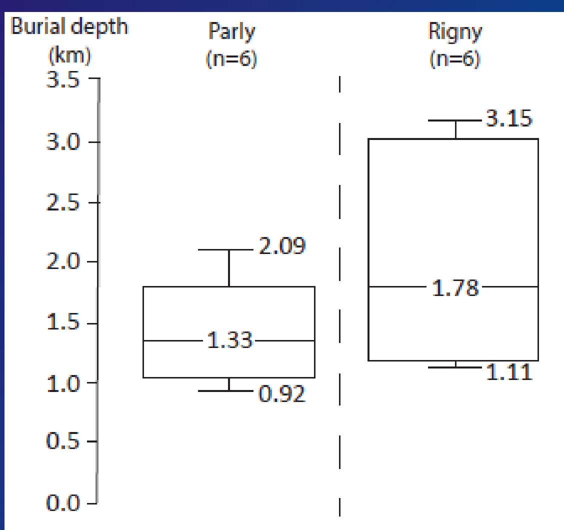

Consistency between maximum burial depth from stylolites and results of basin modelling in the Paris basin

(Beaudoin et al., submitted)

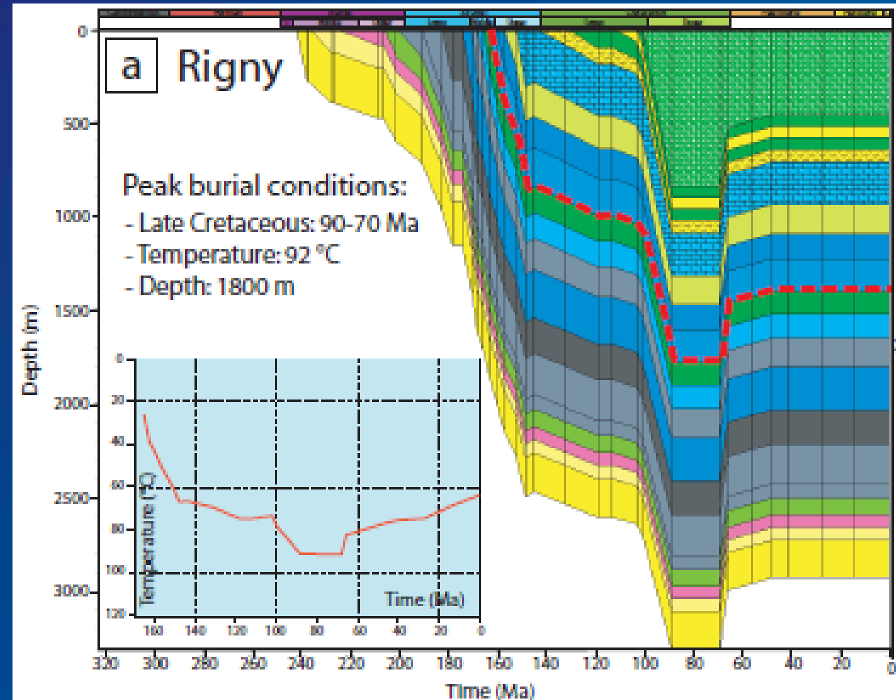

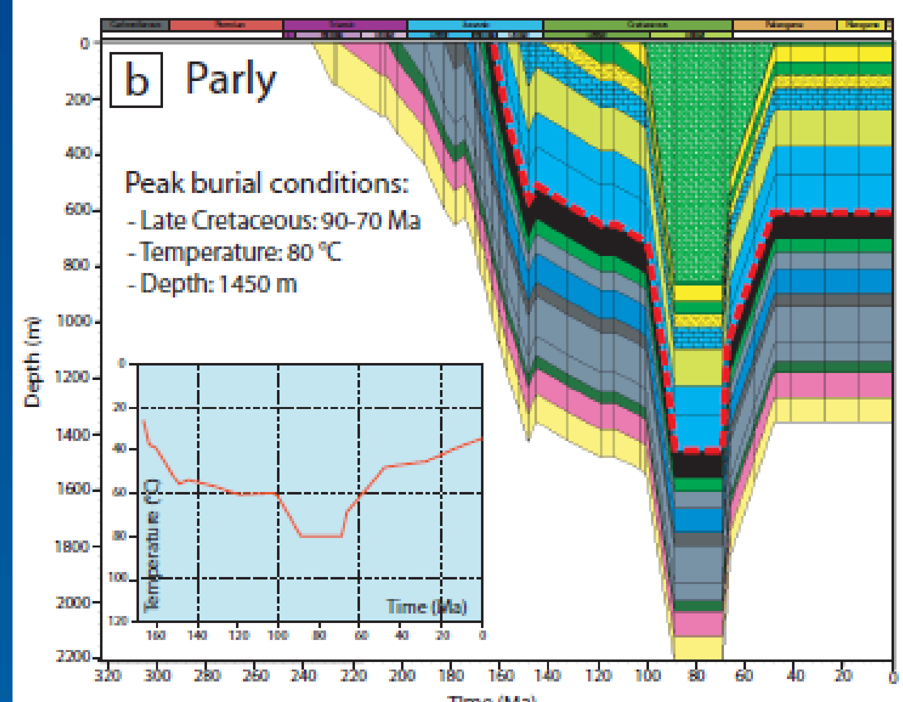

A powerful toolbox : combining calcite twinning and stylolite roughness paleopiezometry

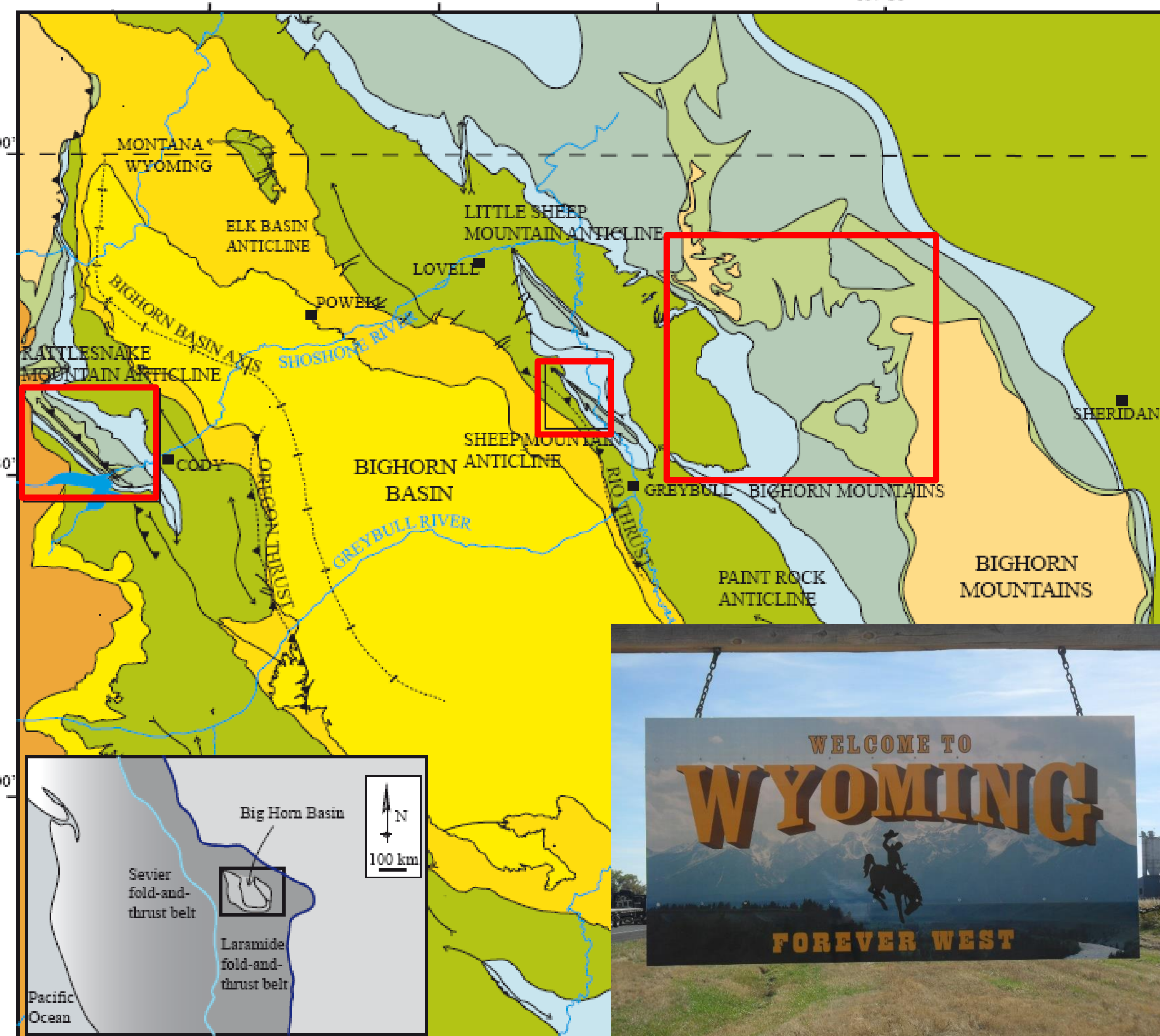
109°00'
108°30'
108°00'
107°30'
45°00'
44°30'
44°00'
MONTANA
WYOMING
ELK BASIN
ANTICLINE
LITTLE SHEEP
MOUNTAIN ANTICLINE
LOVELL
POWELL
BIGHORN BASIN AXIS
SHOSHONE RIVER
RATTLESNAKE
MOUNTAIN ANTICLINE
CODY
OREGON THRUST
BIGHORN
BASIN
SHEEP MOUNTAIN
ANTICLINE
RIO THRUST
GREYBULL
BIGHORN MOUNTAINS
SHERIDAN
GREYBULL RIVER
PAINT ROCK
ANTICLINE
BIGHORN
MOUNTAINS
Big Horn Basin
N
100 km
Sevier
fold-and-
thrust belt
Laramide
fold-and-
thrust belt
Pacific
Ocean
WELCOME TO
WYOMING
FOREVER WEST

Sheep Mountain A.

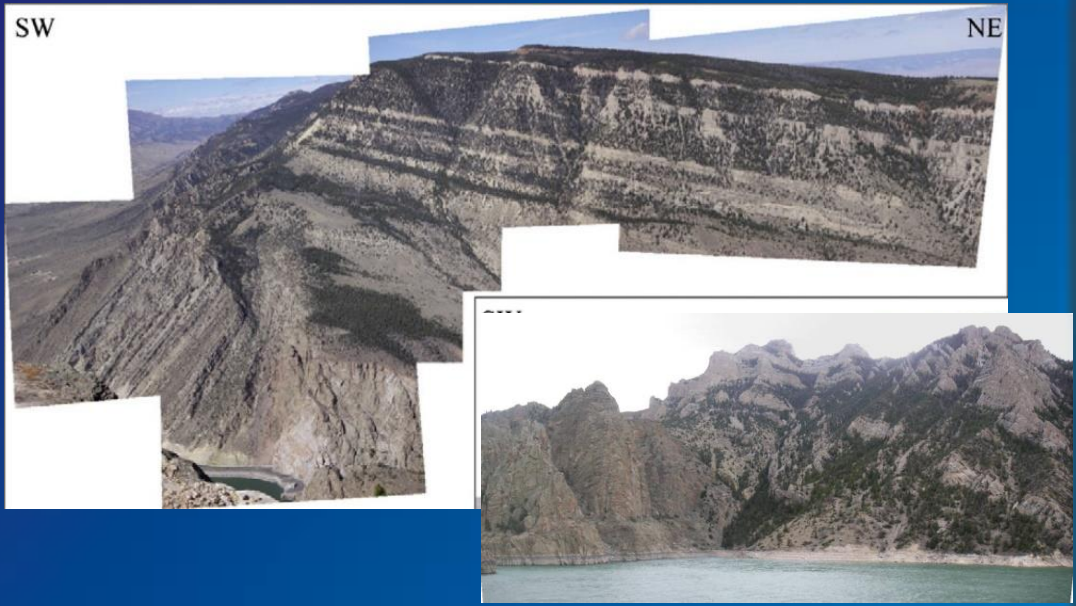

Rattlesnake Mountain A.

BigHorn Mountain A.

Early-folding and late-folding Laramide paleo-differential stress magnitudes from calcite twinning and stylolite roughness paleopiezometry at SMA and RMA

(normalization of RMA to same depth than SMA)

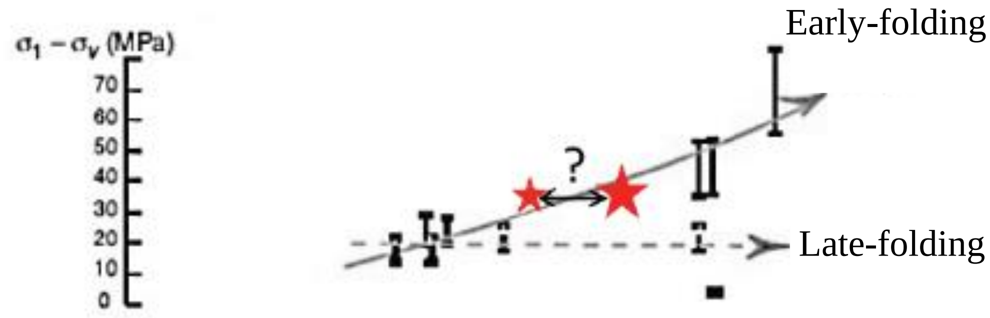

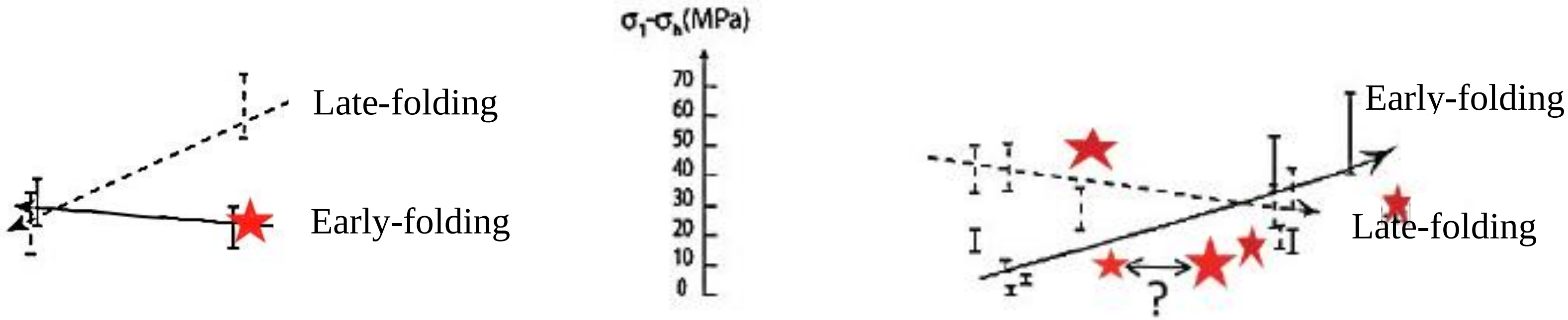

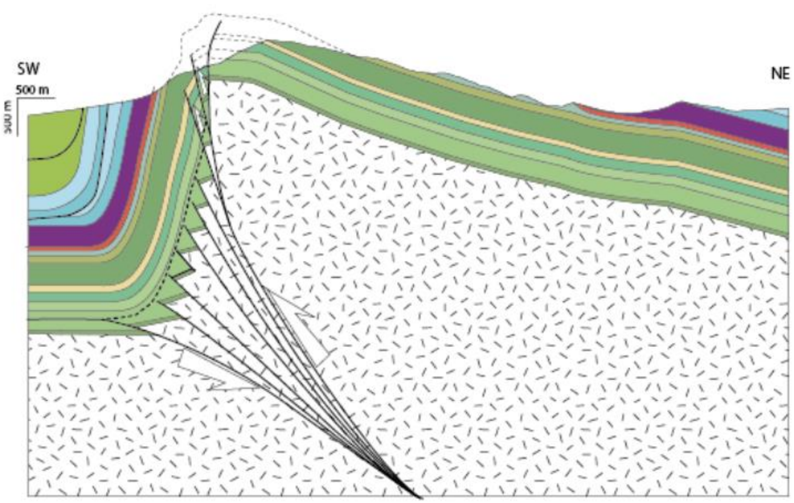

Rattlesnake Mountain A.

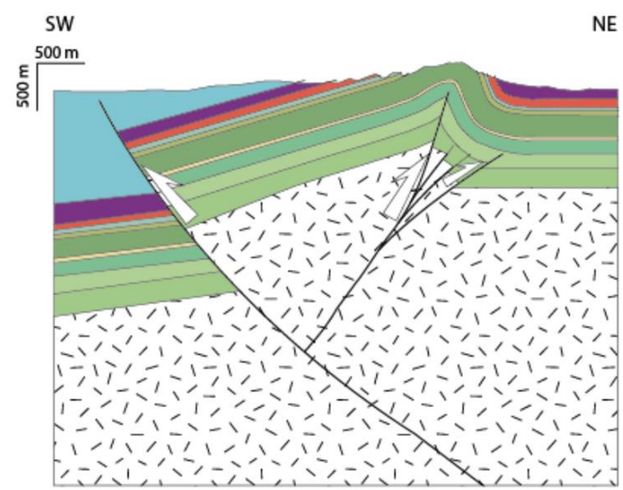

Sheep Mountain A.

Predicted max paleodepth consistent with geological data (independent on T°C)

Stylolite roughness paleopiezometry

Consistent principal stress magnitudes among folds

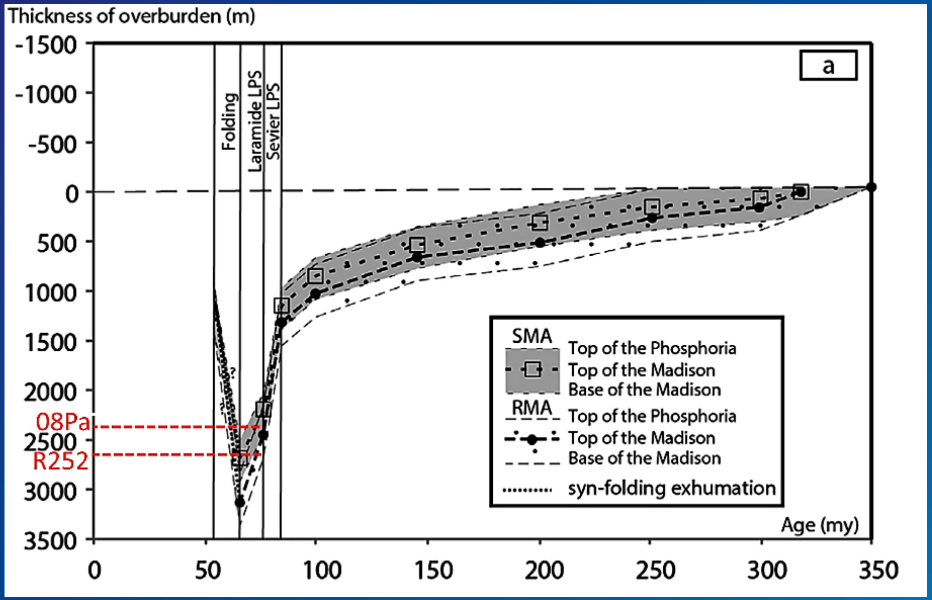

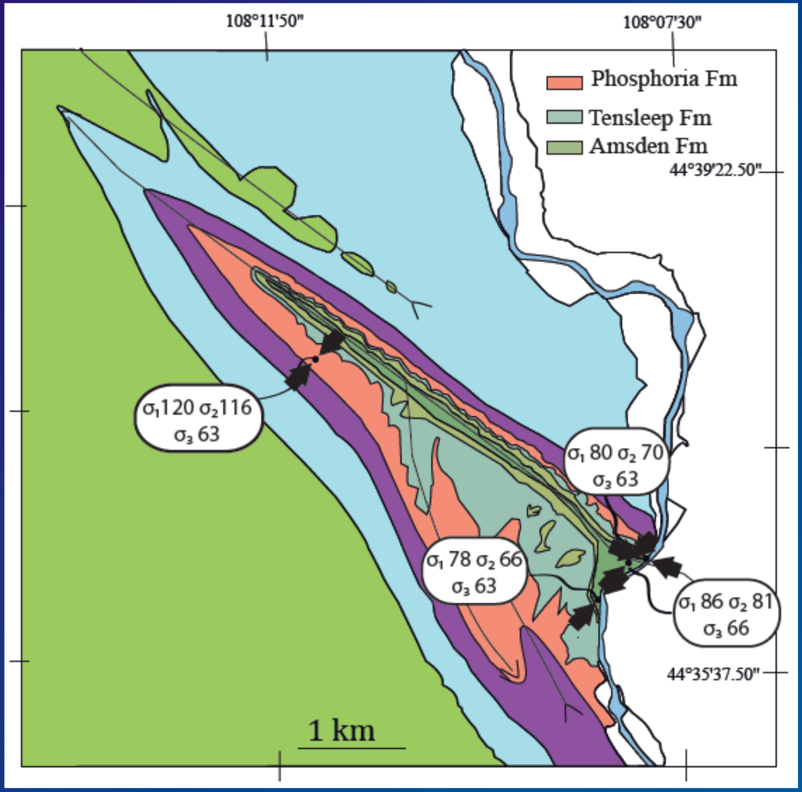

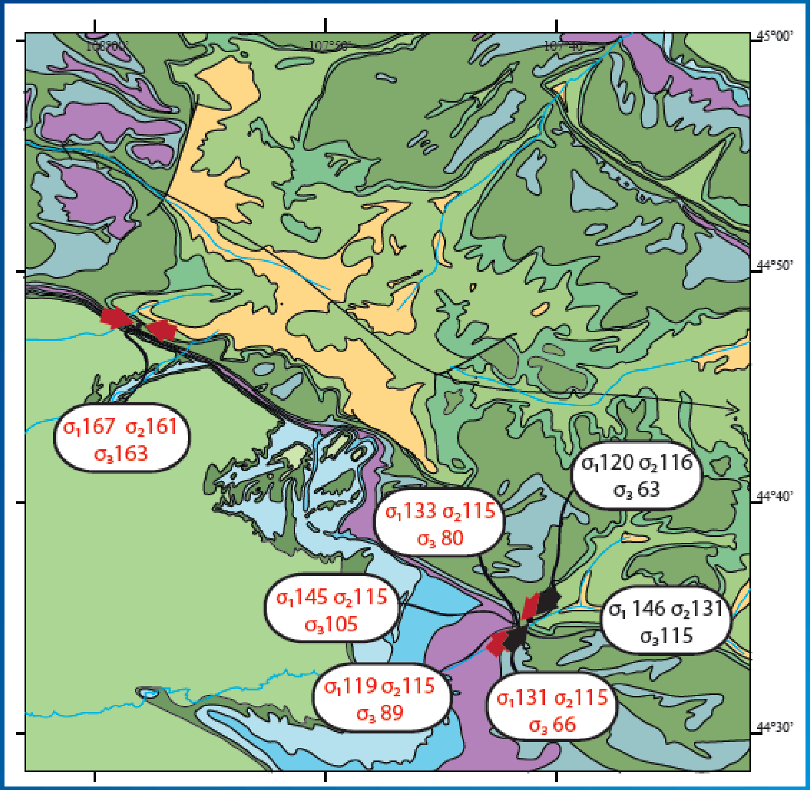

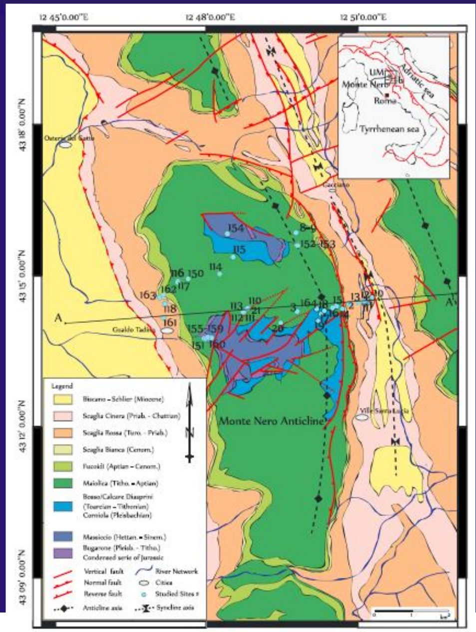

Combining stylolite roughness and calcite twinning paleopiezometry reveals the complexity of progressive stress patterns during folding (Monte Nero anticline, Apennines, Italy

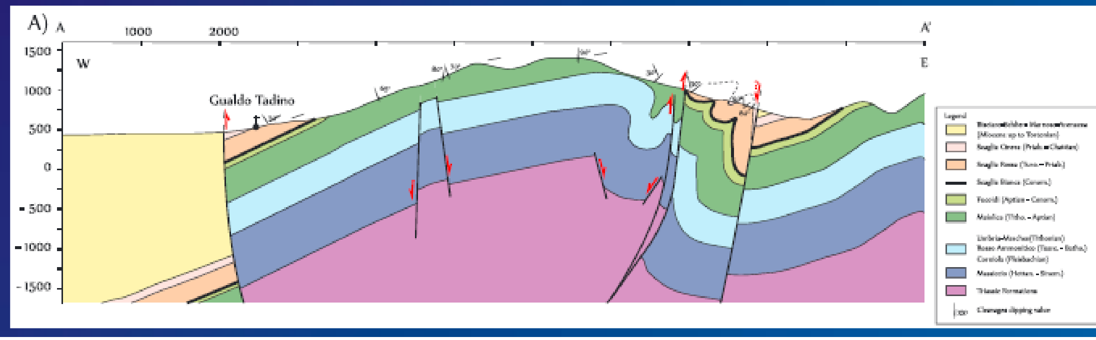

Beaudoin et al., 2016

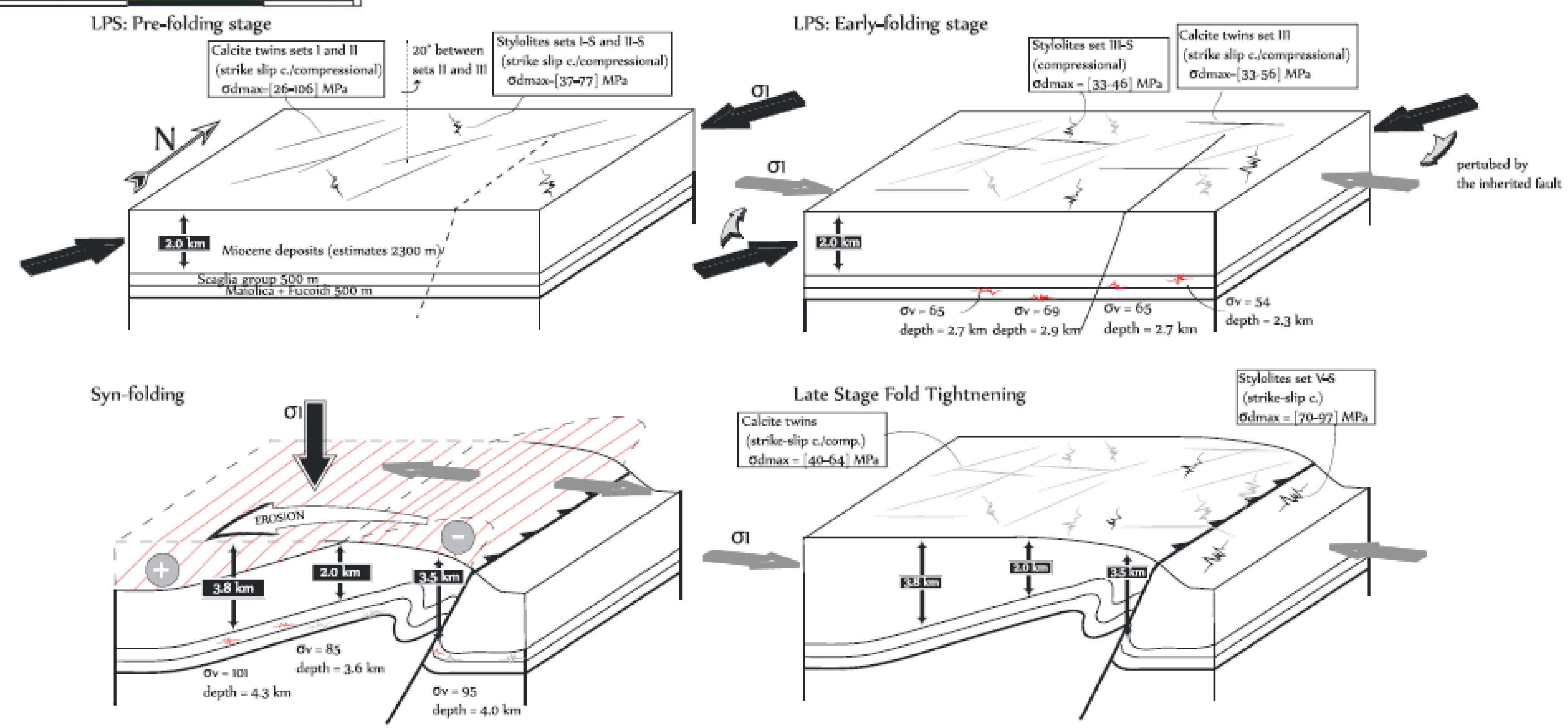

Quantification of principal stress magnitudes and fluid (over)pressures at Sheep Mountain and Rattlesnake Mountain anticlines

Quantifying principal stress magnitudes

Finding for each deformation step, using a simple Mohr construction, the values of σ1, σ2 and σ3 required for consistency between differential stresses estimated from calcite twinning, frictional sliding along preexisting planes (i.e., Byerlee's law) and newly formed faulting/fracturing.

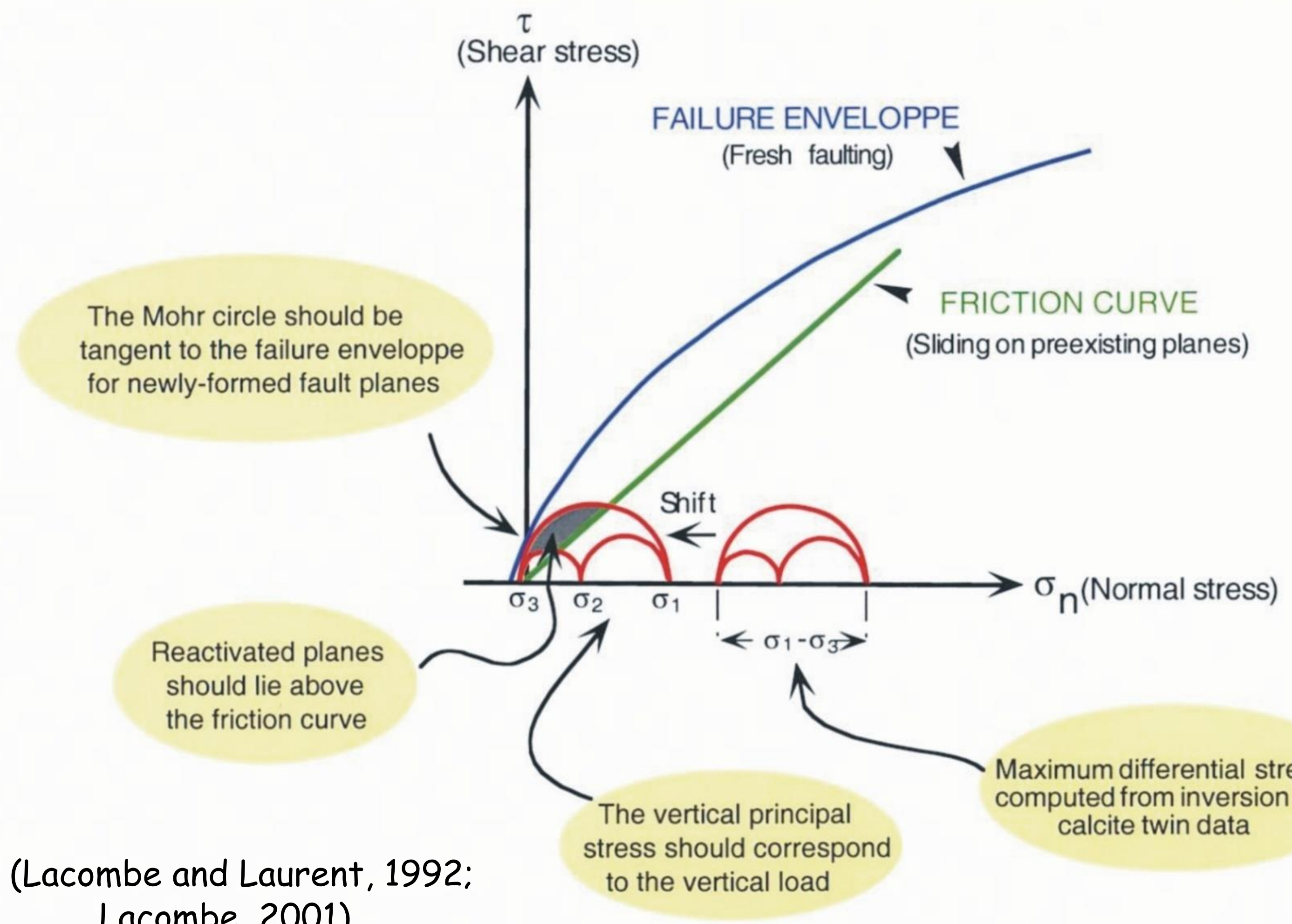

(Lacombe and Laurent, 1992; Lacombe, 2001)

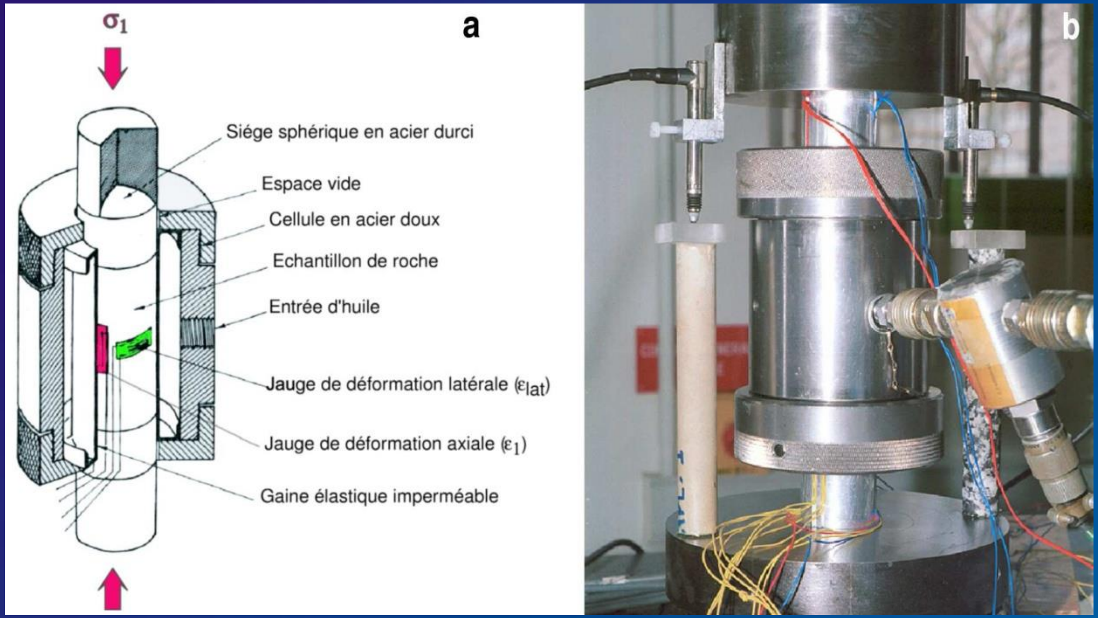

Experimental determination of the intrinsic failure envelopes of the Phosphoria and Madison formations

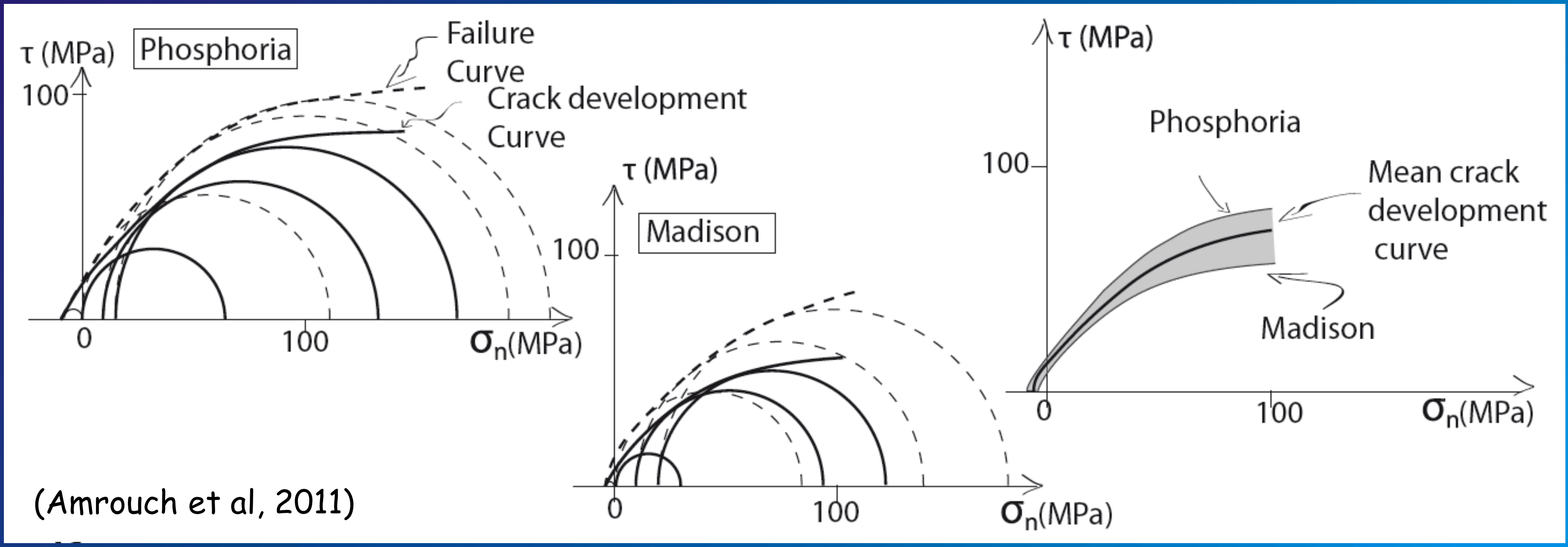

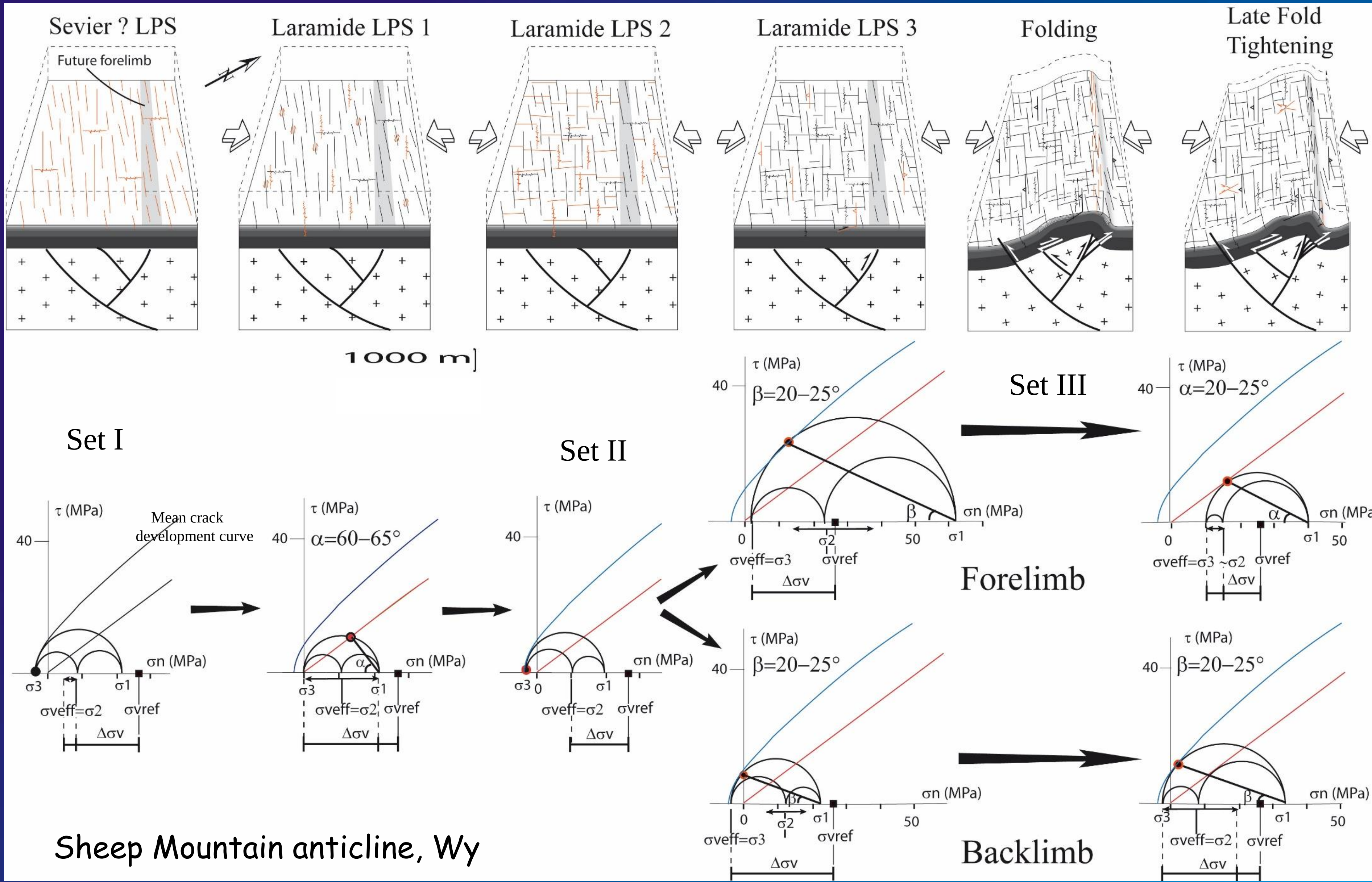

Determination of principal stress magnitudes and $\Delta\sigma_v$ (Amrouch et al, 2011)

Quantifying paleo fluid (over)pressure

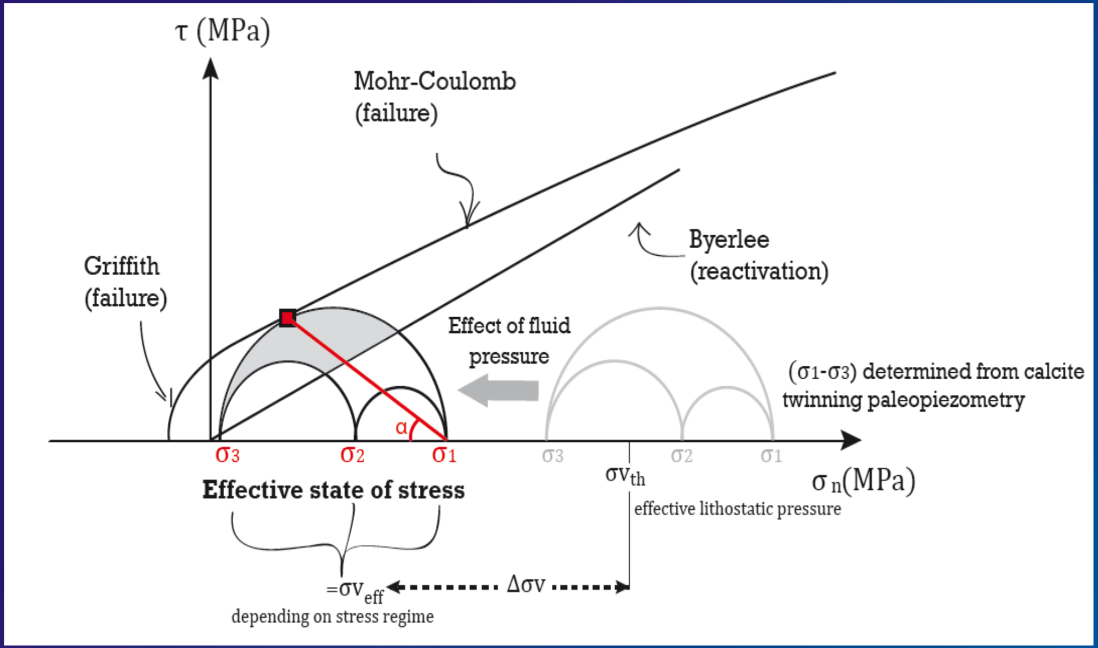

Assumption of a vertical principal stress equal to the effective weight of overburden

Theoretical effective vertical principal stress calculated considering lithostatic pressure corrected from hydrostatic fluid pressure:

$$\sigma_{vref}=(\rho-\rho_w).g.h$$

Comparison between σ_{vref} and the reconstructed effective vertical principal stress σ_{veff} :

$$\Delta\sigma_v=\sigma_{vref}-\sigma_{veff}$$

A non-zero $\Delta\sigma_v$ reflects either fluid over- or under-pressure or burial changes (sedimentation or erosion): when $\Delta\sigma_v$ is positive, either the burial depth was less than the value considered for the calculation of σ_{vref}, or the system was overpressured.

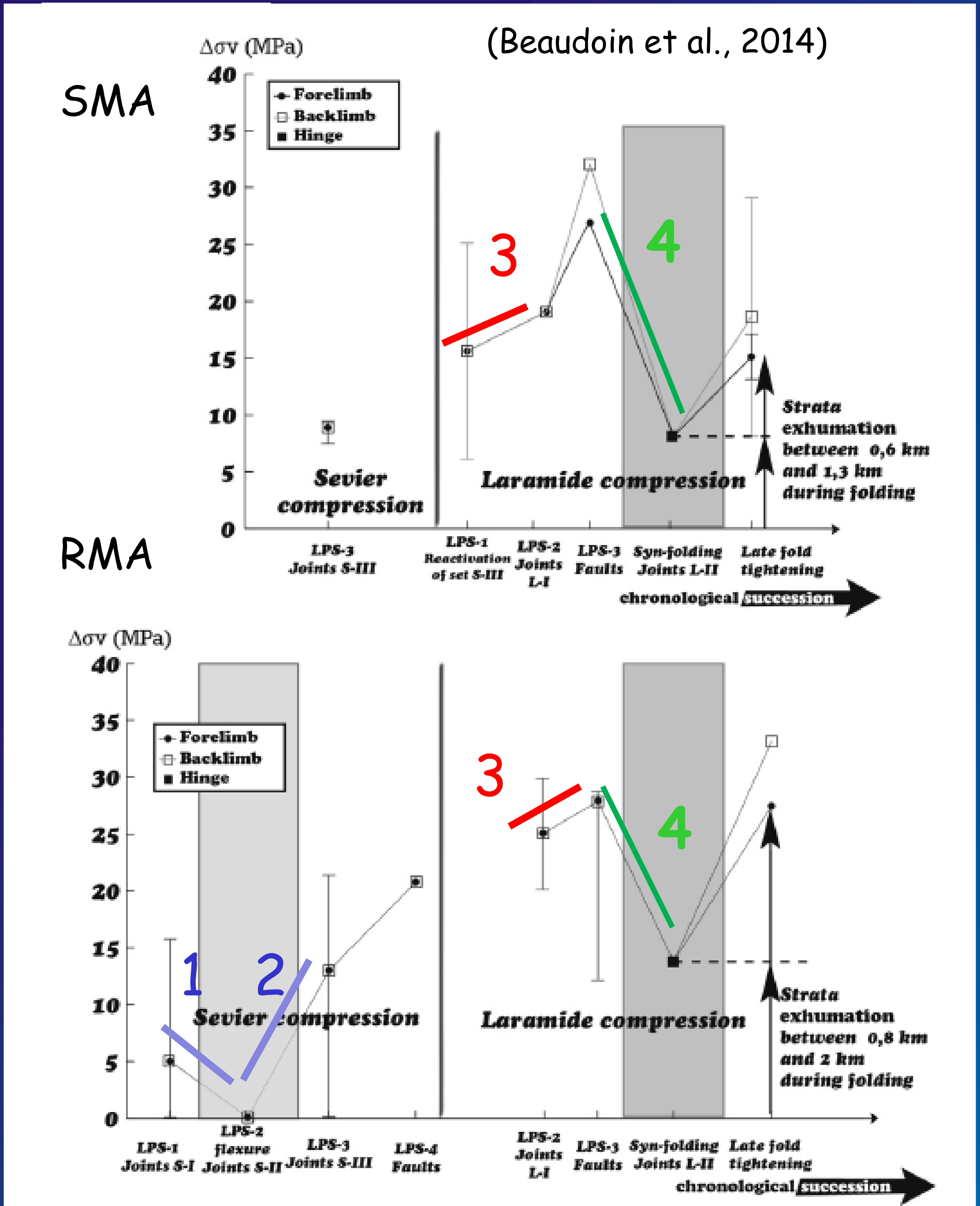

Comparison of $\Delta\sigma_v$ evolution

1. Decrease in fluid overpressure from early Sevier LPS to foreland flexure due to enhanced permeability by flexure-related extensional fractures.

2. Increase during late Sevier-LPS by input of exotic fluids as supported by geochemistry of vein cements.

3.Increase during Laramide LPS due to porosity reduction by pressure-solution/poor hydraulic permeability of fracture sets due to low vertical persistence or to their fast healing/ strong increase in horizontal stress magnitude / input of exotic fluids into the reservoir in response to a large-scale fluid migration.

4. Drop due to development of curvature-related fractures that enhanced the hydraulic permeability of the reservoir. Break of fluid compartmentalization within the Madison-Phosphoria core consistent with geochemistry of syn-folding vein cements that suggests a vertical migration of deeper radiogenic hot fluids within the sedimentary cover.

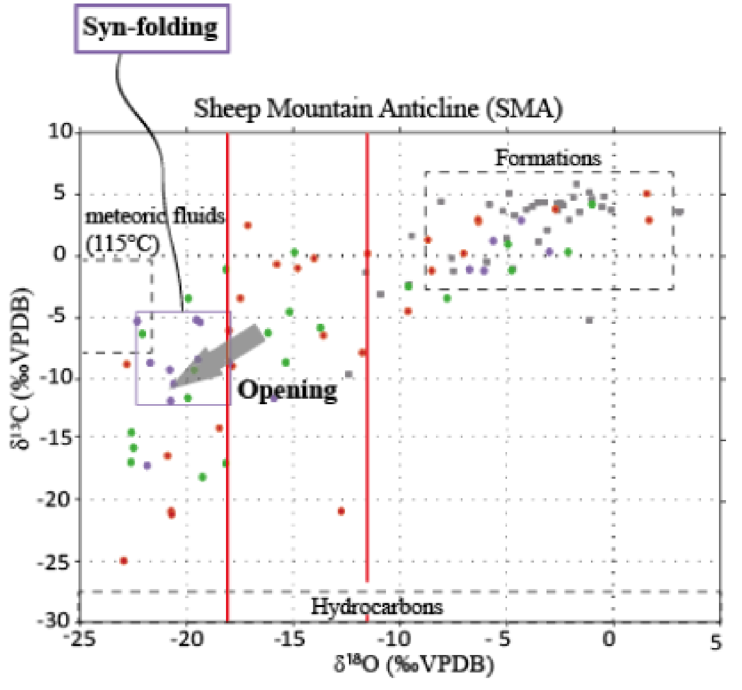

Basement-derived hydrothermal fluid pulse at SMA

Vertical migration of deeper radiogenic hot fluids within the sedimentary cover explained by the development of curvature-related fractures that enhance the hydraulic permeability of the reservoir and break fluid compartmentalization by stratigraphy.

Link with structural style

(Beaudoin et al, 2011; Evans and Fischer, 2012)

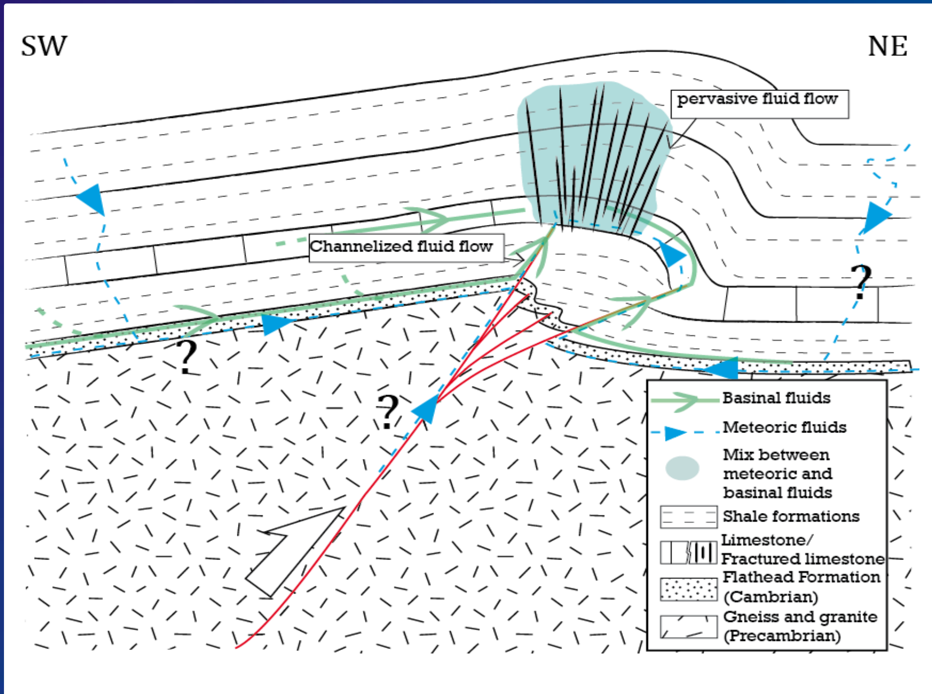

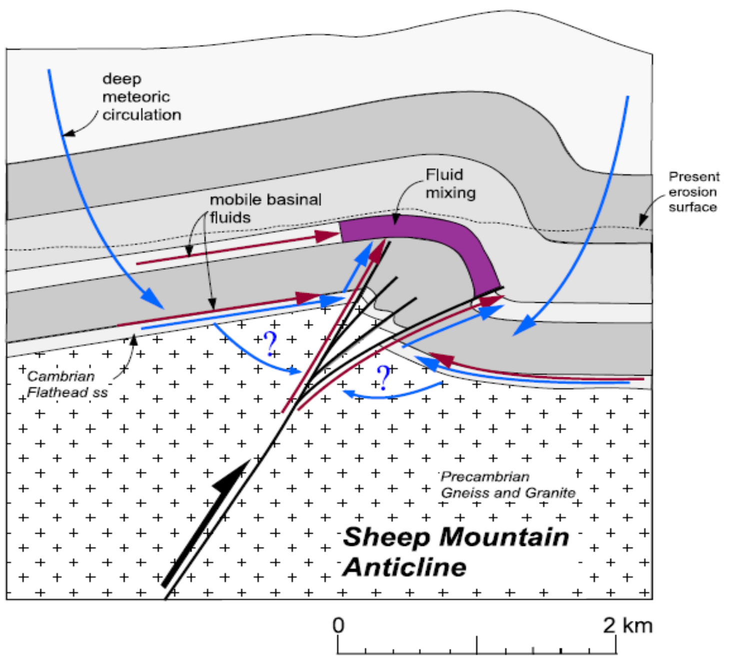

Comparison with values of fluid overpressures in sedimentary basins

derived from paleo-pressure reconstructions based on gas composition in hydrocarbon fluid inclusions or from direct measurements in limestone or shale/sandstone reservoirs.

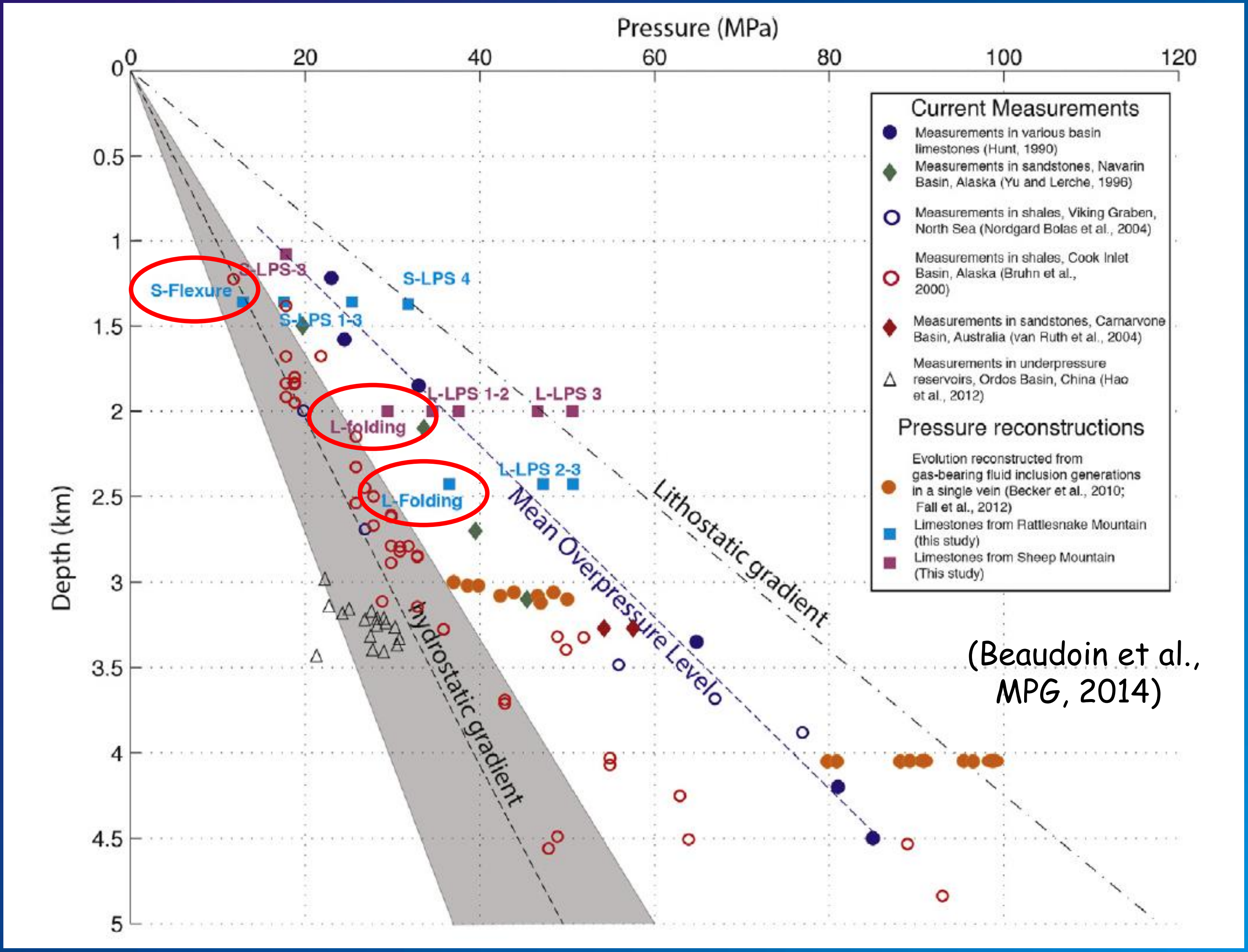

(Beaudoin et al., MPG, 2014)

Take home message

Combining paleopiezometers (e.g., calcite twins / stylolites) : a powerful toolbox that helps constrain …

- stress orientations, regional tectonic history
- values of tectonic (paleo)stress magnitudes
- pore fluid (over) pressure through time in reservoir analogues
- transmission of orogenic stresses to the foreland
- upper crust rheology
- put mechanics into basin/thrust belt kinematic modelling

among others…

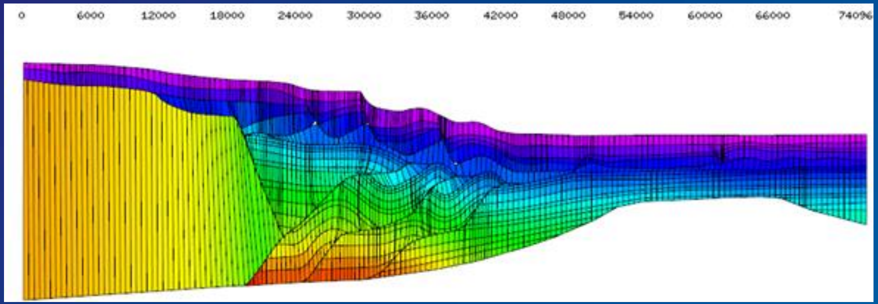

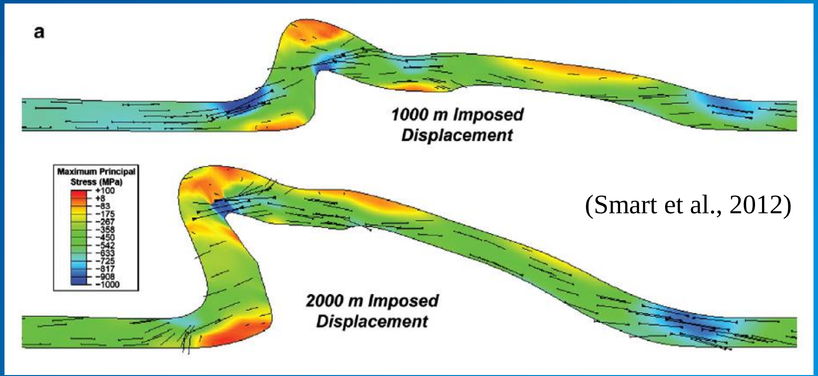

(Smart et al., 2012)

Many thanks for inviting me

Suggested readings :

Amrouch K., Beaudoin N., Lacombe O., Bellahsen N. & Daniel J.M., 2011, Paleostress magnitudes in folded sedimentary rocks. Geophys. Res. Lett., 38, L17301

Beaudoin, N., Koehn. D., Lacombe O., Lecouty A, Billi A., Aharonov., E. & Parlangeau C., 2016. Fingerprinting stress: stylolite and calcite twinning paleopiezometry revealing the complexity of stress distribution during folding – the case of the Monte Nero anticline in the Apennines, Italy. Tectonics, 35, 1687-1712

Beaudoin N., Bellahsen N., Lacombe O., Emmanuel L. & Pironon J., 2014. Crustal-scale fluid flow during the tectonic evolution of the Bighorn Basin (Wyoming, USA). Basin Research, 26, 403–435

Beaudoin N., Lacombe O., Bellahsen N., Amrouch K. & Daniel J.M., 2014. Evolution of fluid pressure during folding and basin contraction in overpressured reservoirs: insights from the Madison-Phosphoria carbonate formations in the Bighorn basin (Wyoming, USA). Marine and Petroleum Geology, 55, 214-229,

Lacombe O., 2001. Paleostress magnitudes associated with development of mountain belts : insights from tectonic analyses of calcite twins in the Taiwan Foothills. Tectonics, 20, 6, 834-849

Lacombe O., 2007, Comparison of paleostress magnitudes from calcite twins with contemporary stress magnitudes and frictional sliding criteria in the continental crust : Mechanical implications. J. Struct. Geol., 29, 86-99

Lacombe O., 2010, Calcite twins, a tool for tectonic studies in thrust belts and stable orogenic forelands. Oil and Gas Science and Technology, 65, 6, 809-838

Calcite twins as low T thermometer

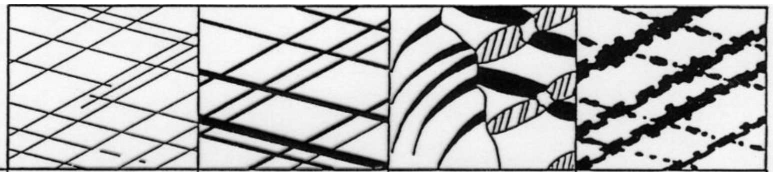

	type I	type II	type III	type IV
Geometry Description	-thin -straight -rational	-thick (>>1μm) -straight -slightly lenseshaped -rational	-curved twins -twins in twins -irrational -completely twinned	-thick, patchy -sutured boundaries -trails of tiny grains -irrational
Interpretations	-little deformation -little cover -low temperature -(post-metamorphic) -(late tectonic)	-considerable def. -completely twinned grains are possible -syn- or post-metamorphic	-large deformation. -intracrystalline def. mechanisms e.g. (r-& f-glide) -syn-metamorphic deformation.	-large deformation -recrystallization (grain boundary migration) -pre- or syn-metamorphic
Temperature	< 200°C	150-300°C	> 200°C	>250°C

Increasing temperature

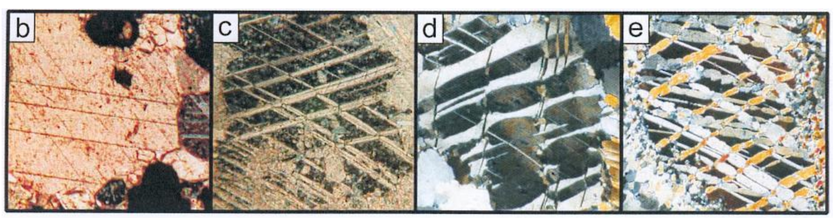

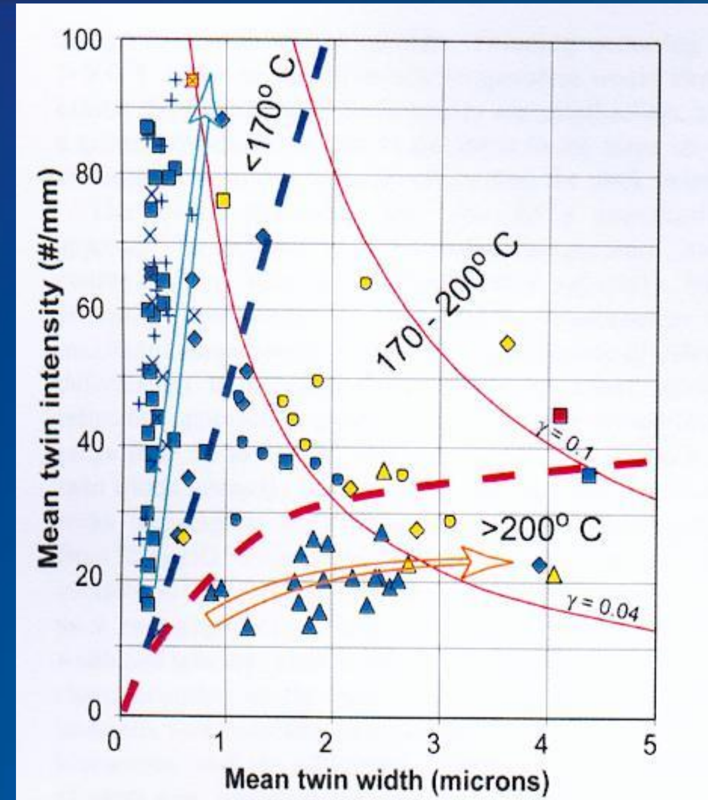

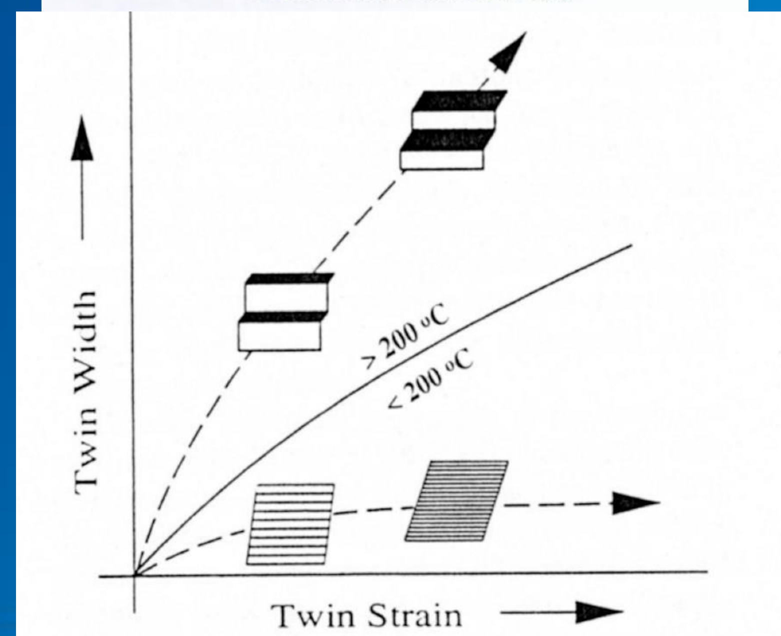

(Burkhard, 1993; Ferrill, 1998; Ferrill et al., 2004)

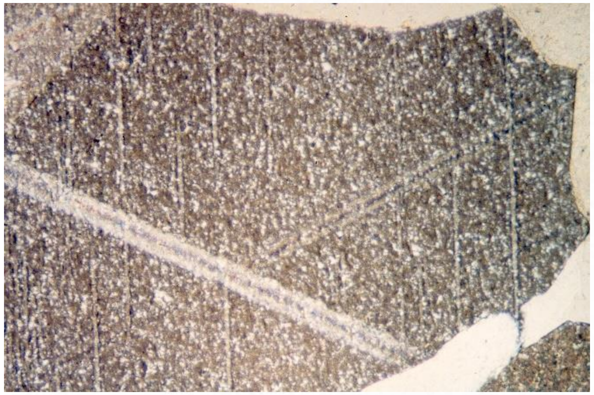

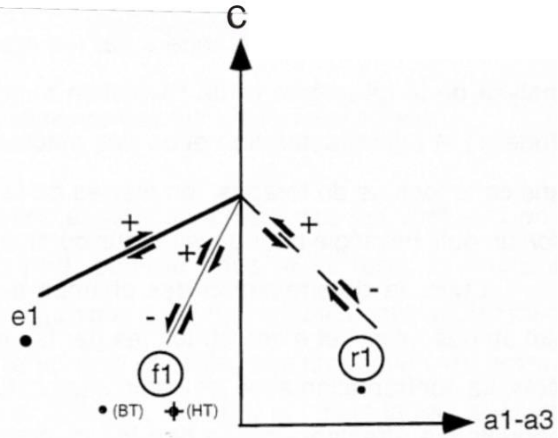

e-twinning and r, f-gliding systems in calcite

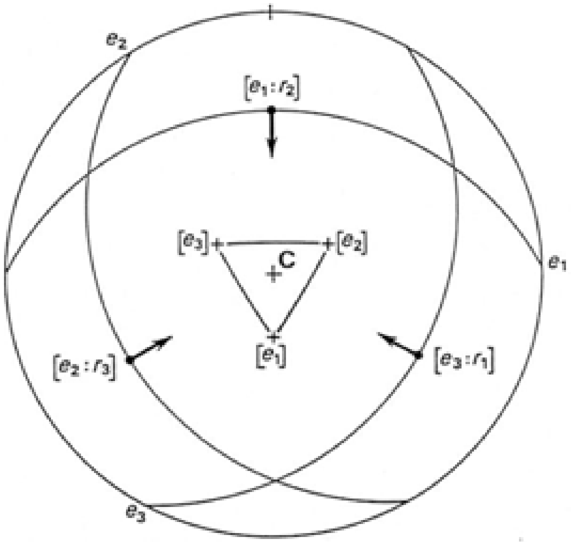

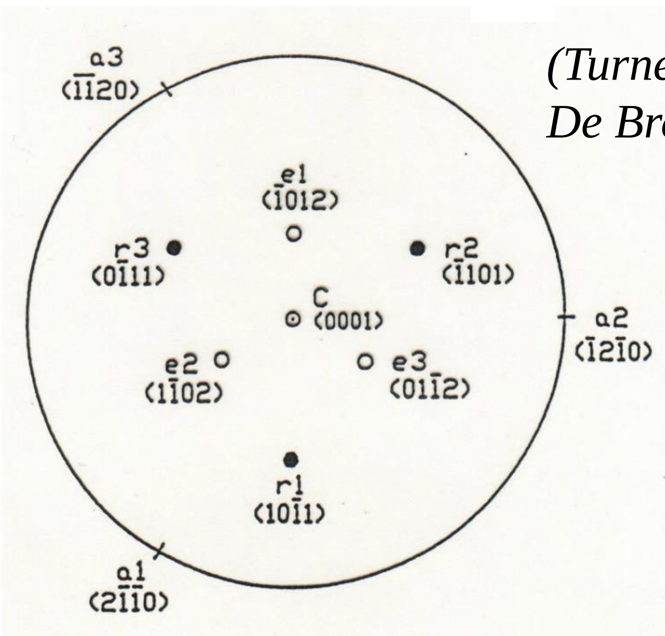

(Turner and Weiss, 1976; De Bresser et al., 1997)

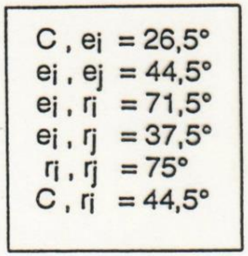

Data acquisition using EBSD

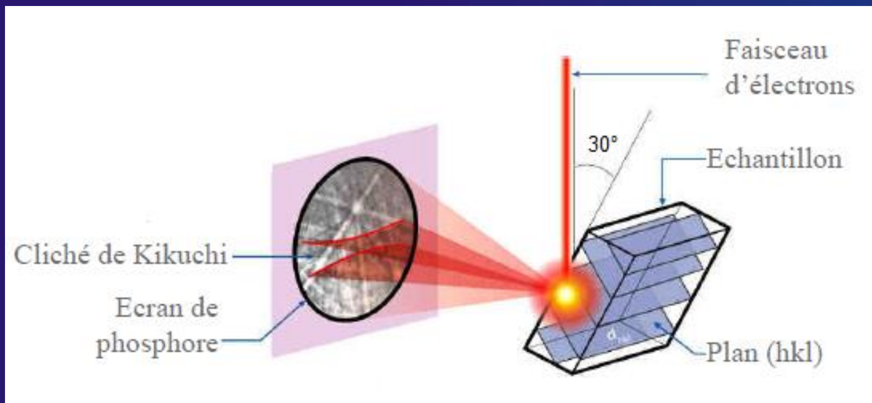

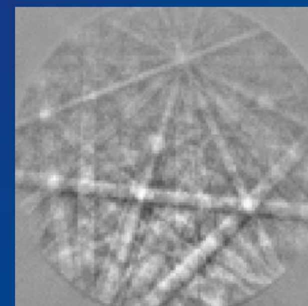

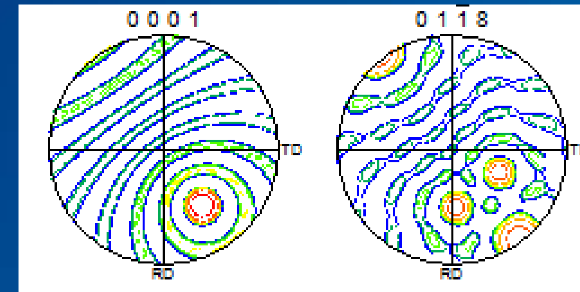

Twin lamella

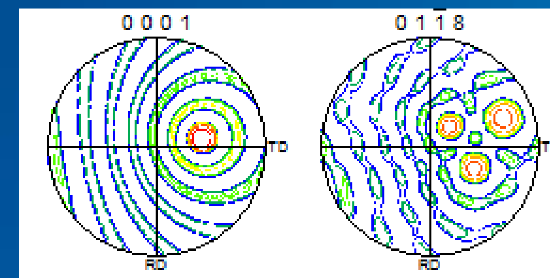

Host crystal

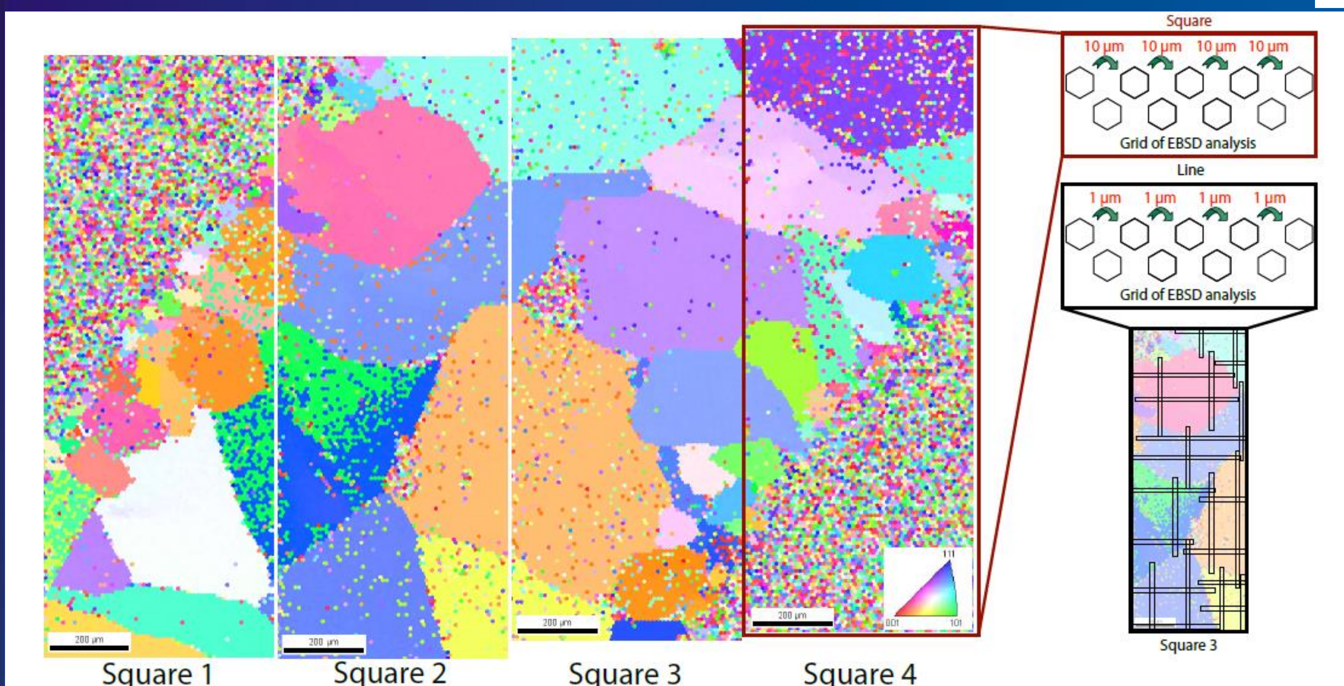

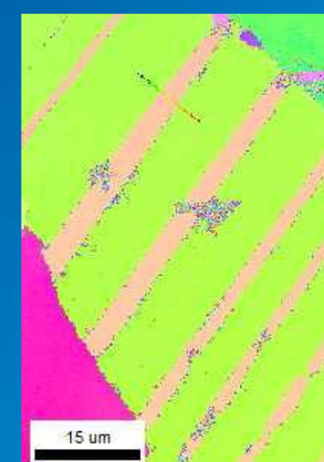

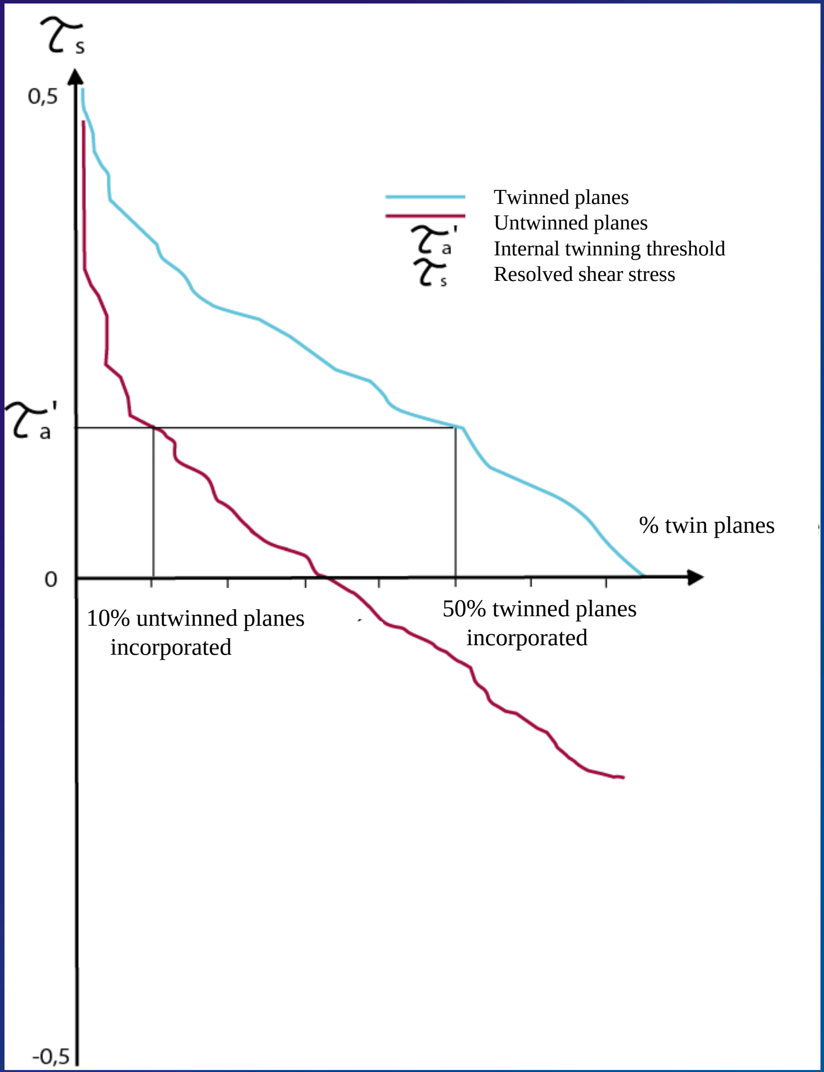

τ_s
0,5
Twinned planes
Untwinned planes
τ_a' Internal twinning threshold
τ_s Resolved shear stress
τ_a'
% twin planes
0
10% untwinned planes incorporated
50% twinned planes incorporated
-0,5

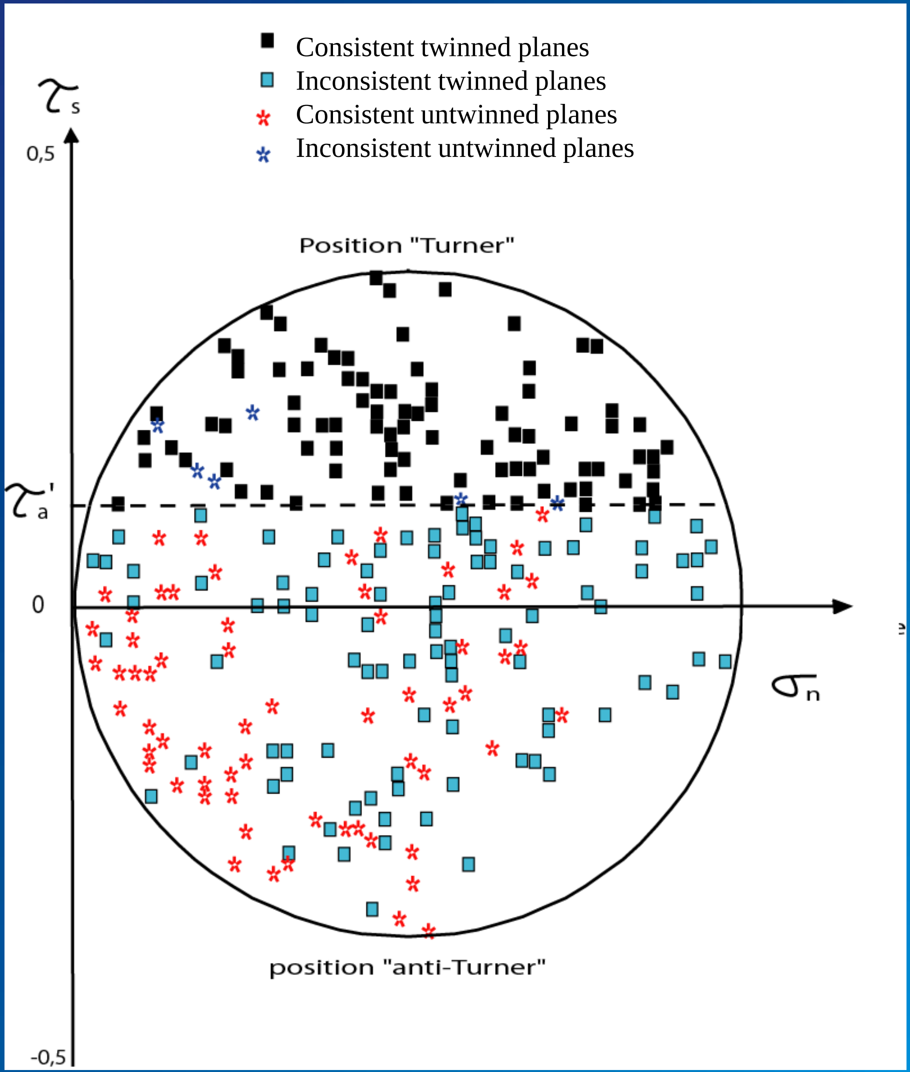

Consistent twinned planes
Inconsistent twinned planes
Consistent untwinned planes
Inconsistent untwinned planes
τ_s
0,5
Position "Turner"
τ_a'
0
σ_n
position "anti-Turner"
-0,5

Influence of grain size

(Rowe and Rutter, 1990)

Slope = twin density,
does not depend on grain size

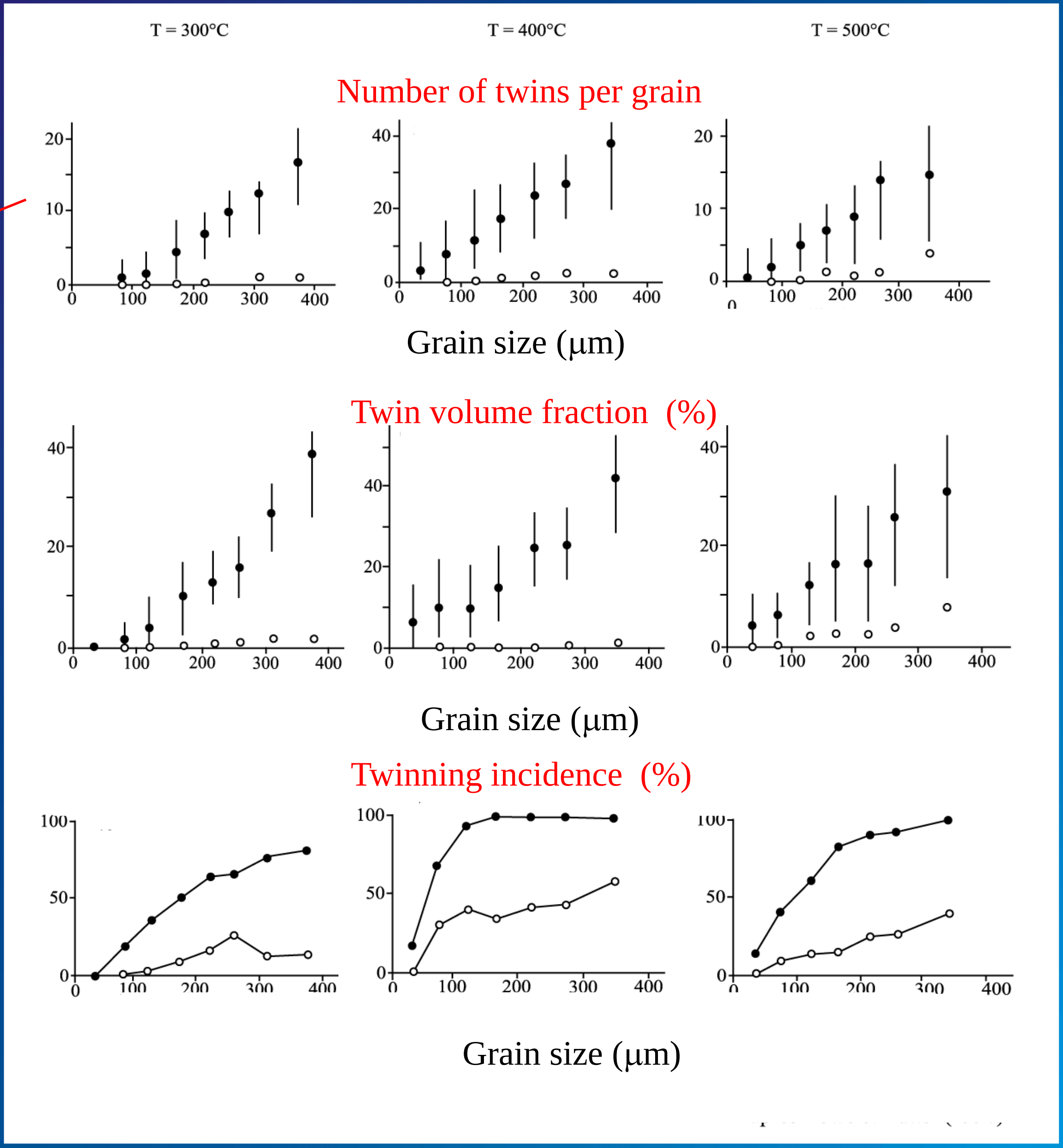

Estimates of syn-folding erosion

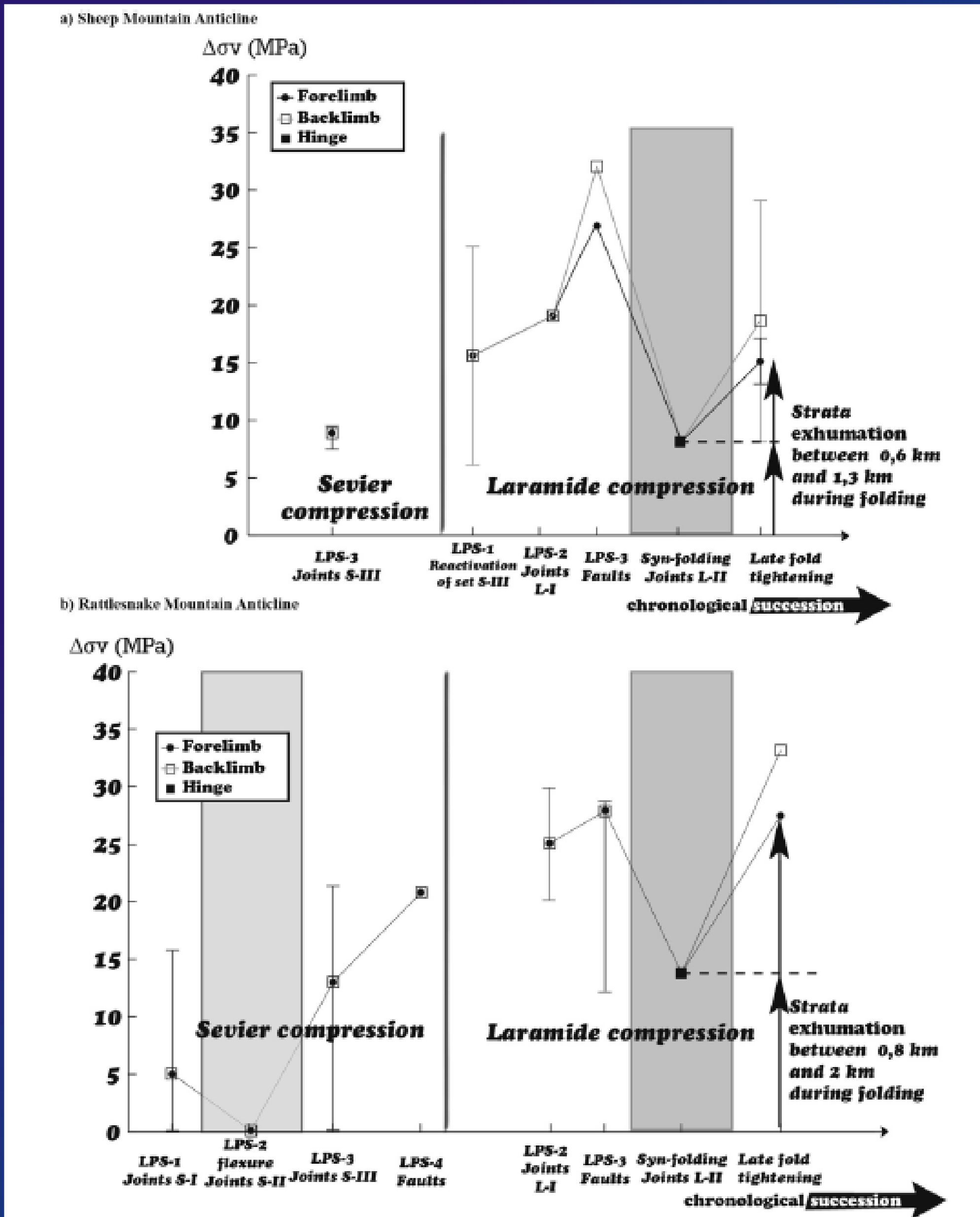

The post-folding Δ_{sv} value can be used to calculate the eroded/ burial thickness E as well as the post-folding overburden thickness H

$$E = \Delta_{sv} / [(\rho_{rock} - \rho_{water})g]$$

$$H = [\sigma_{vth} - \Delta_{sv}] / [(\rho_{rock} - \rho_{water})g]$$

The high Δ_{sv} value recorded during the LSFT suggests exhumation of the strata, consistent with the development of topography during folding.

Drastic drop in fluid pressure during folding :
-either a hydrostatic fluid pressure prevailed in the reservoir → exhumation :1.3/ 2km at SMA/RMA
-or a supra-hydrostatic fluid pressure still persisted after folding (overpressure not totally released) → syn-folding value of Δ_{sv} reflects the remaining fluid overpressure
→ exhumation : 0.6/0.8 km at SMA/RMA

Assuming a syn-folding erosion of 0.6-2.0 km and a duration of folding of 5-20 Ma → exhumation rate by folding of 0.03-0.40 mm/yr, consistent with exhumation/rock uplift rates in other Laramide arches derived from LT thermochronology and paleoelevation/basin analyses.

Koehn et al., 2016

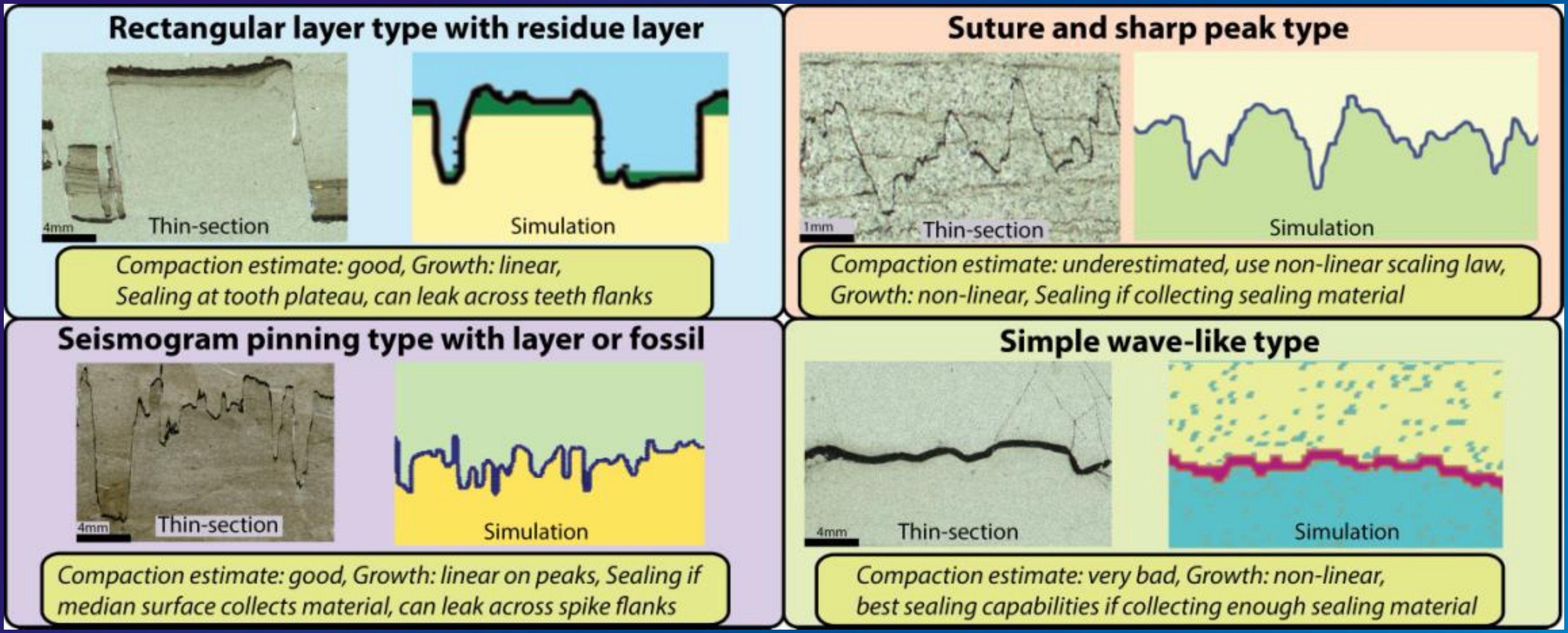

Stylolite types suitable for paleostress estimates : must display small-scale and large-scale amplitudes

-Suture and sharp peak (III)

-Seismogram (II) if one considers the morphology in between the large teeth that reflect pinning rather than dissolution

- Simple wave (IV) provided they display two wavelengths

Stylolites are very common rough dissolution surfaces

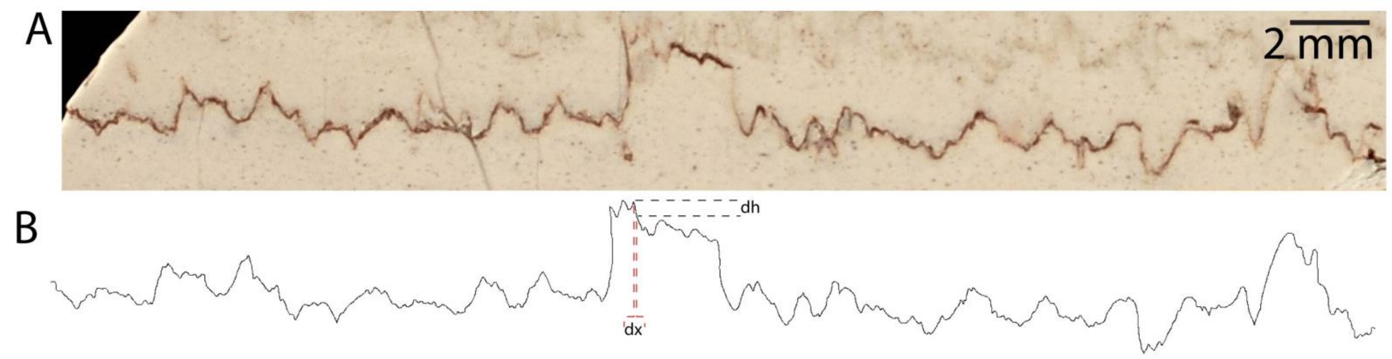

They can be used to:

1. *Estimate the direction of the main compressive stress*
2. *Estimate burial depth*
3. *Estimate tectonic stresses*

Vitesse de dissolution à l'interface (Rolland et al., 2012) :

$$v_d = Ts - \frac{l}{L_c} I_e + \eta$$

Ts : Tension de surface prenant en compte les effets induits par la courbure de la surface.
I_e : Interactions élastiques décrivant la déformation de la surface.
η : désordre présent dans la roche (hétérogénéités) et dont les variables sont indépendantes du temps.

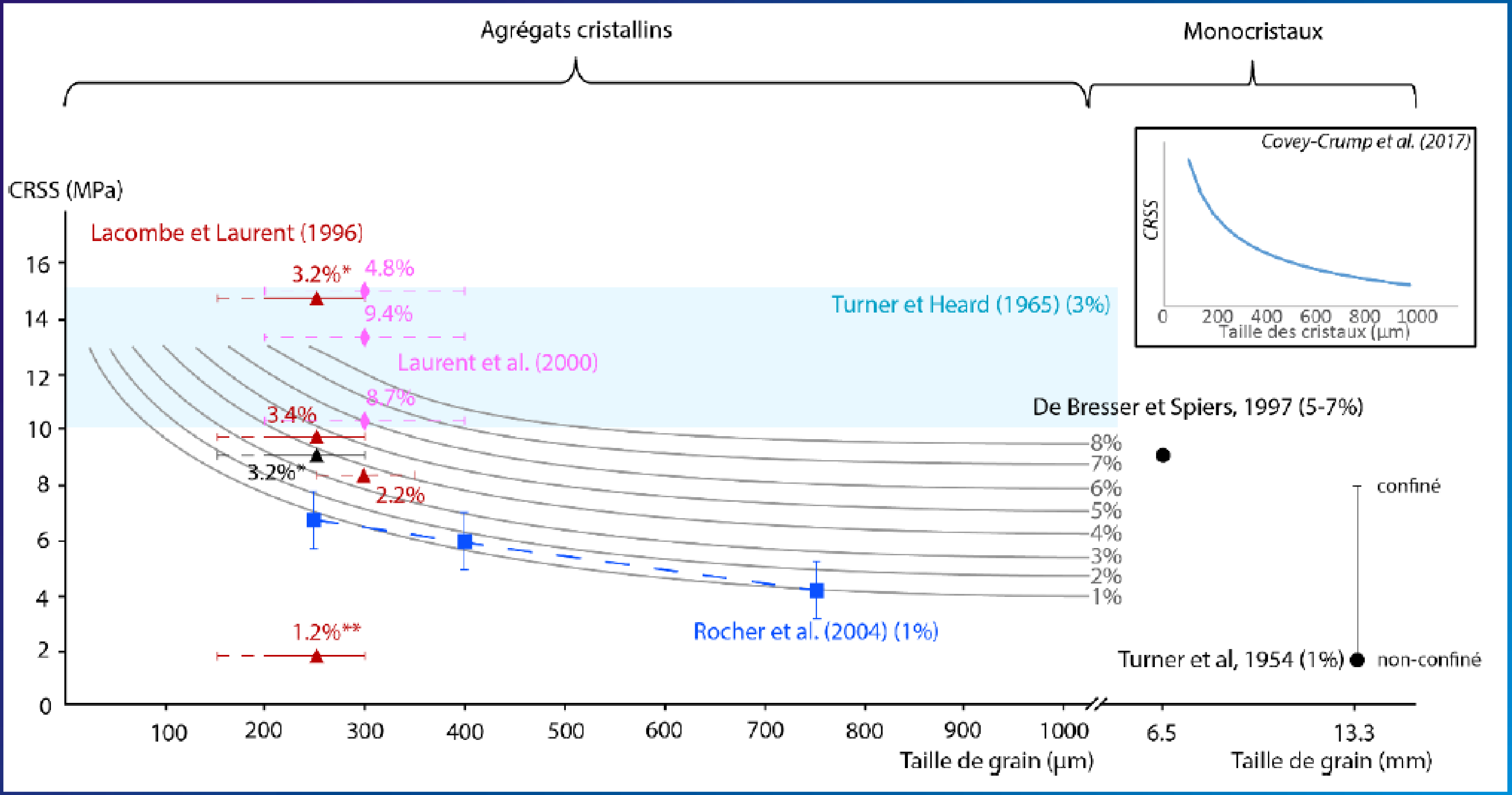

(Parlangeau, 2017)

Evolution of fluid system in SMA and RMA

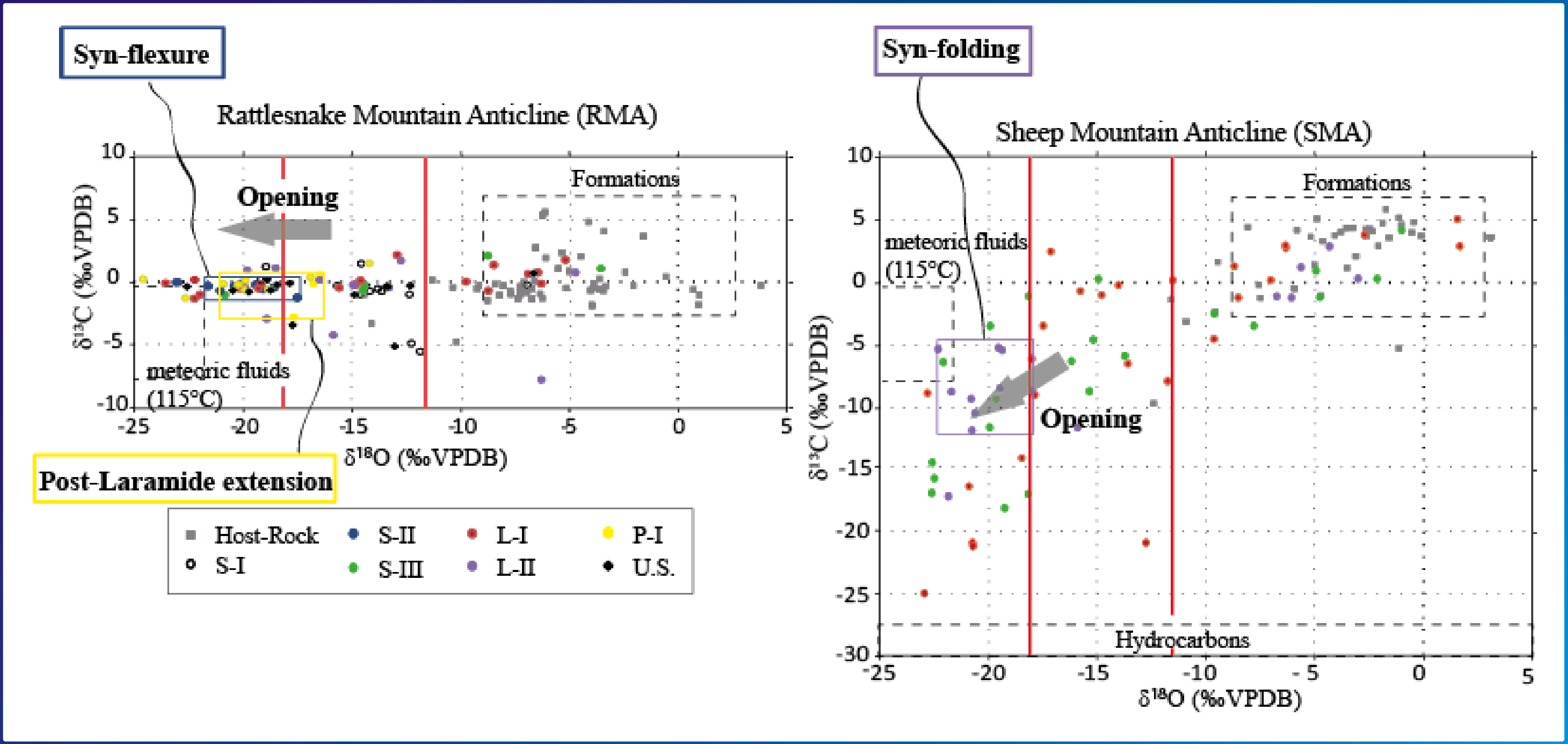

Stress perturbations in the sedimentary cover at the tip of the underlying basement fault starting to move during Laramide stress build-up

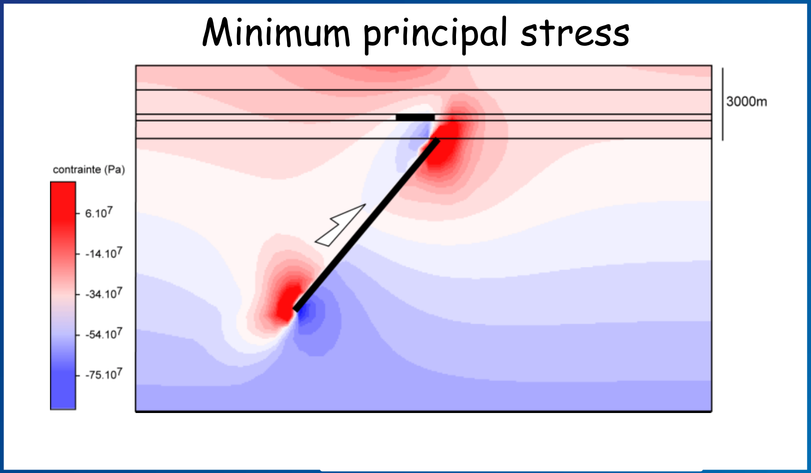

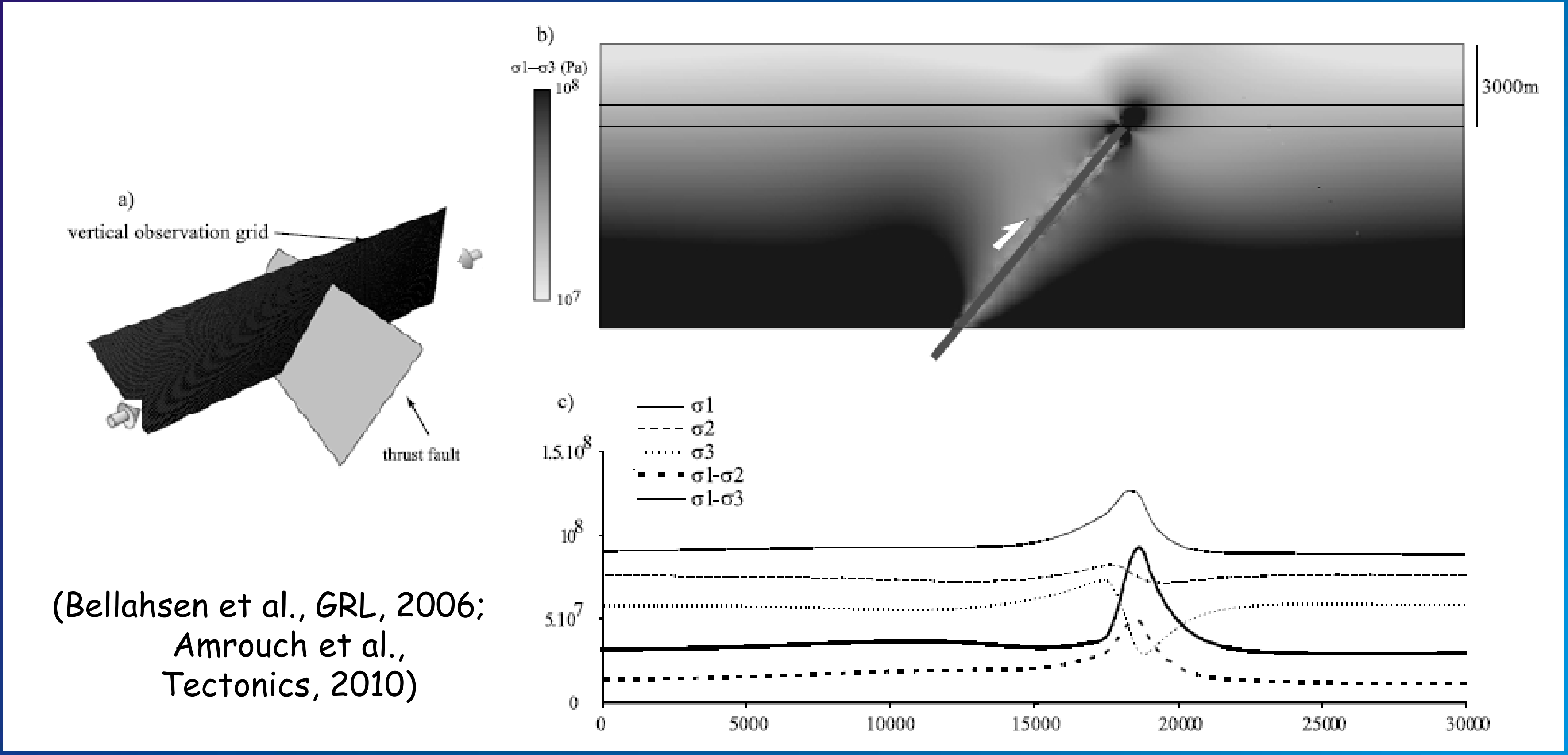

(Bellahsen et al., GRL, 2006; Amrouch et al., Tectonics, 2010)